Modelling aerosol molecular markers in a 3D air quality model: Focus on anthropogenic organic markers

Grazia Maria Lanzafame, Bertrand Bessagnet, Deepchandra Srivastava, Jean Luc Jaffrezo, Olivier Favez, Alexandre Albinet, Florian Couvidat

Modelling aerosol molecular markers in a 3D air quality model: focus on anthropogenic organic markers.

Grazia Maria Lanzafame[a, b], Bertrand Bessagnet[a, b, 1], Deepchandra Srivastava[a, 2], Jean Luc Jaffrezo[c], Olivier Favez[a], Alexandre Albinet[a], and Florian Couvidat[a, *]

[a]INERIS, Parc Technologique Alata, BP 2, 60550 Verneuil-en-Halatte, France

[b]Sorbonne Universités, UPMC, 75252 PARIS cedex 05, France

[c]University of Grenoble Alpes, CNRS, IRD, INP-G, IGE (UMR 5001), F-38000 Grenoble, France

[1]Now at European Commission, Joint Research Centre (JRC), Ispra, Italy

[2]Now at School of Geography Earth and Environmental Science, University of Birmingham, Birmingham, B15 2TT, UK

Highlights (3 to 5 bullet points, maximum 85 characters, including spaces, per bullet point).

- Anthropogenic organic marker formation mechanism inserted in a 3D air quality model

- Comparison of model outputs with gaseous and particulate phase field measurements

- Underestimation of some markers suggests missing emissions or formation pathways

- Modelled partitioning mainly hydrophilic and gas-phase fraction overestimation

- Constant modelled levoglucosan/OC ratio observed only for high OM concentrations

Abstract.

We developed and implemented in the 3D air quality model CHIMERE the formation of several key anthropogenic aerosol markers including one primary anthropogenic marker (levoglucosan) and 4 secondary anthropogenic markers (nitrophenols, nitroguaiacols, methylnitrocatechols and phthalic acid). Modelled concentrations have been compared to measurements performed at 12 locations in France for levoglucosan in winter 2014-15, and at a sub-urban station in the Paris region over the whole year 2015 for secondary molecular markers. While a good estimation of levoglucosan concentrations by the model has been obtained for a few sites, a strong underestimation was simulated for most of the stations especially for western locations due to a probable underestimation of residential wood burning emissions. The simulated ratio between wood burning organic matter and particulate phase levoglucosan is constant only at high OM values (>10 µg m^{-3}) indicating that using marker contribution ratio may be valid only under certain conditions. Concentrations of secondary markers were well reproduced by the model for nitrophenols and nitroguaiacols but were underestimated for methylnitrocatechols and phthalic acid highlighting missing formation pathways and/or precursor emissions. By comparing modeled to measured Gas/Particle Partitioning (GPP) of markers, the simulated partitioning of Semi-Volatile Organic Compounds (SVOCs) was evaluated. Except for nitroguaiacols and nitrophenols when ideality was assumed, the GPP for all the markers was underestimated and mainly driven by the hydrophilic partitioning. SVOCs GPP, and more generally of all SVOC contributing to the formation of SOA, could therefore be significantly underestimated by air quality models, especially when only the partitioning on the organic phase is considered. Our results show that marker modelling can give insights on some processes (such as precursor emissions or

2

missing mechanisms) involved in SOA formation and could prove especially useful to evaluate the GPP in 3D air quality models.

1. Introduction and objectives

Air quality models are numerical tools used to forecast air pollution and evaluate air quality control policies. By using data such as emissions and meteorology, chemistry transport models (CTMs) simulate the main processes involved in the evolution of pollutant concentrations in the atmosphere. However, the model performances depend strongly on the model parametrizations and configurations inducing that simulation results from different models are often discordant (Bessagnet et al., 2016).

Organic aerosol (OA) is a major fraction of the fine particulate matter (PM) (Bressi et al., 2021; Kanakidou et al., 2005; Zhang et al., 2011, 2007) originating from both anthropogenic and biogenic sources. Whereas primary organic aerosols (POA) are directly emitted into the atmosphere, secondary organic aerosols (SOA) are produced by atmospheric (photo-) chemical reactions. Their formation occurs via oxidation of the volatile and semi-volatile organic compounds (VOCs and SVOCs) leading to the formation of products of lower volatility that partition between the gaseous and particulate phases. SOA formation depends on multiple factors (reactant concentrations, meteorological parameters, emission sources…) and its representation in air quality model remains challenging (Carlton et al., 2009; Hallquist et al., 2009; Heald et al., 2010; Kroll and Seinfeld, 2008; Ziemann and Atkinson, 2012).

Due to the great number of organic species, emissions sources (biomass burning, road traffic, vegetation, etc….) and processes involved in OA formation (aqueous-phase reactions, gas-phase reactions, oligomerization, gas/particle partitioning), it is not straightforward to

3

validate modelling results by comparison to in-situ OA observations and to understand the reasons of a lack of performances of air quality models. Previous work using near-explicit chemistry simulations in remote environments demonstrated the importance to consider the chemical speciation to model properly OA formation (Roldin et al., 2019; Xavier et al., 2019). To improve OA modelling, it seems essential to perform molecular scale simulations and therefore to implement in detailed chemical mechanisms, the associated physicochemical processes and the emissions of OA precursors. Modelling molecular OA tracers (markers) could be used to improve the knowledge on OA and study the involved phenomena via the representation of detailed chemical reactions. Using such an approach, the performances of air quality models, the influence of chemical mechanisms, physicochemical processes and OA precursor emission can be investigated using a molecular approach (Li et al., 2021; Wilson et al., 2020; Zhang et al., 2021).

Several molecular markers from specific sources (or SOA precursors) have been reported in the literature and are used for source apportionment purposes (Hopke et al., 2020; Karagulian et al., 2015; Kleindienst et al., 2007; Lanzafame et al., 2021; Schauer et al., 1996; Srivastava et al., 2021, 2019, 2018b, 2018c, 2018a). For instance, levoglucosan is commonly used as a primary marker for biomass burning emissions (Bhattarai et al., 2019; Simoneit et al., 1999) and constant ratios between the wood burning organic matter (OM_{wb}) and particulate phase levoglucosan, estimated by measurement data, are often used to evaluate the contribution of wood-burning aerosol to organic aerosol (Herich et al., 2014; Puxbaum et al., 2007; Schmidl et al., 2008).

Nitrated phenolic compounds (nitrophenols, nitroguaiacols and methylnitrocatechols) are photooxidation products of biomass burning VOCs (Forstner et al., 1997; Iinuma et al., 2010; Lauraguais et al., 2014; Olariu et al., 2002; Yee et al., 2013) even if some of them have also

4

been detected in primary biomass burning emissions (Lu et al., 2019; Wang et al., 2017). Phthalic acid has been proposed as a marker for naphthalene and methylnaphthalenes photooxidation (Kleindienst et al., 2012). However, it has also been observed as a degradation product of phthalates emitted by plastic materials (Hankett et al., 2013) and it might be directly emitted by vehicular engines (Kawamura and Kaplan, 1987). Although all the PM source apportionment marker-based methods assume that these compounds are stable in the atmosphere and mainly associated to the particulate phase, they can be degraded in atmosphere by sunlight and by reaction with atmospheric radicals (Nozière et al., 2015; Srivastava et al., 2018b). In addition, evidences of their semi-volatile behavior have been provided by different authors (Al Naiema and Stone, 2017; Bannan et al., 2017; Booth et al., 2012; Lanzafame et al., 2021; Xie et al., 2014; Yee et al., 2013).

One of the challenges to include gas/particle partitioning (GPP) in 3D air quality models is to evaluate their thermodynamic properties such as the subcooled liquid saturated vapor pressure (P_{sat}) and the vaporization enthalpy (ΔH_{vap}). Only a few studies have evaluated anthropogenic marker thermodynamic properties and their partitioning in ambient air and their outcomes are often discordant (Bannan et al., 2017; Bilde et al., 2015; Booth et al., 2011; Oja and Suuberg, 1999; Xie et al., 2014). For simplification purposes, aerosol models often assume the ideality whereas the partitioning is strongly dependent on non-ideality (Couvidat et al., 2012, Kim et al., 2019). Moreover, aerosol viscosity affects the diffusion of the organic species inside the particle, slowing down the exchange processes with the gaseous phase (Shrivastava et al., 2017). Kim et al. (2019) showed that considering the viscosity of the organic phase could lead to a strong increase of particle-phase concentrations of semi-volatile compounds.

A few recent studies have focused on the 3D modelling of anthropogenic molecular markers. Li et al. (2021) have simulated the global distribution of levoglocusan concentrations with the GEOS-CHEM model (Bey et al., 2001). The authors concluded that statistical parametrizations derived from the 3D simulation results may be used to account for the atmospheric degradation in levoglucosan measurements. These parameterizations could be used to improve their use for quantitative aerosol source apportionment. Zhang et al. (2021) implemented the formation of 2,3-Dihydroxy-4-oxopentanoic acid (DHOPA, a marker of monoaromatic compounds) in CMAQ (Byun and Schere, 2001) by using chamber-derived mass yields. They managed to reproduce the field measurements of DHOPA with a mean fractional bias of 15.2%. The authors emphasize that simulating DHOPA in air quality models could be used to refine the quantification of SOA attributable to monoaromatic hydrocarbons.

This paper focuses on the development and implementation of chemical formation mechanisms, on the GPP simulation for some anthropogenic molecular markers (levoglusosan and several secondary SOA molecular markers: nitrophenols, nitroguaiacols, methylnitrocatechols and phthalic acid) in a 3D CTM and on the model evaluation by comparison with the measurements. Sensitivity simulations have been performed to understand the influence of the molecular interactions on the aerosol formation and partitioning. A modelling study on levoglucosan to OM ratio variation has been also performed to assess the possibility to use constant ratios to apportion OM_{wb}. The measurement database used includes wintertime (2014-2015) data in 10 French sites and annual (2015) data from a rural site in the Eastern France for levoglucosan. For both, levoglucosan and secondary molecular markers, annual (2015) measurement data from a suburban site located in the Paris region were used.

2. Model development

A gas phase mechanism for the formation of molecular markers in ambient air has been developed and inserted in the 3D chemistry-transport model CHIMERE 2017β including an aerosol module (Couvidat et al., 2018). Briefly, CHIMERE uses a sectional approach, with particles separated into 9 bins from 10 nm to 10 μm. The evaporation/condensation of semi-volatile compounds is represented (Pandis et al., 1993) using thermodynamic equilibria computed with the thermodynamic modules ISORROPIA for inorganics and the secondary organic aerosol processor for organics (SOAP) (Couvidat and Sartelet, 2015; Fountoukis and Nenes, 2007). The model considers the coagulation of particles (Debry et al., 2007), the wet and dry deposition of particles as a function of their wet diameter (Couvidat et al., 2018) and H_2SO_4 nucleation (Kulmala et al., 1998).

The molecular marker formation mechanisms have been added to the gas-phase mechanism MELCHIOR2 and to the Hydrophilic/Hydrophobic Organics (H^2O) SOA formation mechanism already inserted in CHIMERE (Couvidat et al., 2012; Derognat et al., 2003). In the H^2O mechanism, SOA are produced by the photooxidation of the major VOCs (isoprene, monoterpenes, sesquiterpenes, toluene and xylene). POA is treated as SVOCs and split in 3 surrogate species with different volatility and aging products. Here, and as described previously (Majdi et al., 2019), the H^2O mechanism has been refined by adding SOA formation from the oxidation of several precursors namely, phenol, cresol, catechol, benzene, guaiacol, syringol, naphthalene.

2.1 Overview of the molecular marker mechanisms

The molecular marker version of CHIMERE includes 236 species and 639 reactions, against the 69 species and 215 reactions in the original version.

For secondary anthropogenic molecular markers, the precursors considered were benzene, toluene, guaiacol and phenol. Mechanisms for molecular markers formation were sought in literature, taken from the Master Chemical Mechanism (MCM, version 3.3.1) and missing information were produced using the Generator for Explicit Chemistry and Kinetics of Organics in the Atmosphere (GECKO-A) for the gaseous phase chemistry (Camredon et al., 2007). These mechanisms were developed with the following procedure: the reaction intermediates were photolyzed, oxidized or hydrolyzed according to kinetics and branching ratios obtained from laboratory data. When laboratory data were not available, the reactivity was estimated by analogy with similar better characterized systems or with structure activity relationships (SARs). Further reaction steps considered also the reactivity with HO_2, RO_2, NO and NO_2, photolysis, hydrolysis.

The detailed mechanisms for anthropogenic molecular markers are discussed and reported in the supplementary material (SM, section S1). Briefly, toluene, benzene, phenol and cresol photooxidation mechanisms were taken from MCM, in which nitrophenol and methylnitrocatechol formation mechanisms are entirely described. Nitroguaiacols were generated from guaiacol by a two-step nitration mechanism (Coeur-Tourneur et al., 2010; Lauraguais et al., 2014; Yang et al., 2016) and were modelled as the sum of the 3-,4- and 6-nitroguaiacol (see section S1.2). According to Lauraguais et al., (2014), 4-nitroguaiacol is the major nitroguaiacol isomer produced in atmosphere from the OH-initiated photooxidation (63% of the total nitroguaiacols produced by the OH-initiated photooxidation of guaiacol) and is the only isomer measured in this study. Since no isomer specific yield from the NO_3-initiated photooxidation has been provided in the literature, it is not possible to estimate properly 4-nitroguaiacol percentage in the total nitroguaiacols. Phthalic acid formation from naphthalene

oxidation has been modelled according to the mechanism proposed by Kautzman et al., (2010).

The gas/particle partitioning of molecular markers was computed with SOAP (Couvidat and Sartelet, 2015). Here, the GPP was estimated by the model using P_{sat} and ΔH_{vap}. These parameters have been sought in literature. All the thermodynamic properties of the molecular markers considered here are summarized in Table 1. Experimental data have been preferred when available. For the molecular markers with no available data, SARs estimations have been inserted in the model or used to deduce semi-empiric values related to experimental data for similar molecules. Henry's law constants (K_H) used for marker deposition have been calculated with SOAP.

Table 1 Thermodynamic properties of the modelled anthropogenic molecular markers. P_{sat} and ΔH_{vap} are used as input to calculate ΔH_{vap} and K_H with SOAP (Couvidat and Sartelet, 2015).

Modelled species	Molecular markers	P_{sat} at 298K (torr)	ΔH_{vap} (KJmol^{-1})	K_H at 298 K (M^{-1} atm)
LEVO	Levoglucosan	1.45×10^{-6}	52.0	2.26×10^{10}
MNCATECH	Methylnitrocatechols*	3.20×10^{-6}	41.7	1.30×10^{9}
NGUAIACOL	4-Nitroguaiacol	4.61×10^{-5}	30.9	5.60×10^{7}
NPHEN	Nitrophenols**	3.86×10^{-5}	51.2	3.90×10^{7}
PHTHALIC	Phthalic Acid	1.26×10^{-5}	40.0	1.20×10^{8}

*Sum of 3-methyl-5-nitrocatechol, 4-methyl-5-nitrocatechol and 3-methyl-6-nitrocatechol. Thermodynamic properties of a generic methylnitrocatechol.
**Sum of 2-nitrophenol and 4-nitrophenol. Thermodynamic properties of 4-nitrophenol.

2.1.1 Marker GPP computation

In SOAP, the user chooses whether the SVOC species are hydrophilic (condensed onto the aqueous phase of particles), hydrophobic (condensed onto the organic phase) or both (condensed on both phases). By using the molecular structure assigned to each species, the model computes the activity coefficients in order to consider non-ideality with the UNIversal Functional group Activity Coefficient model (UNIFAC) for short-range interactions

(interactions between solvent species) (Fredenslund et al., 1975) and the Aerosol Inorganic–Organic Mixtures Functional groups Activity Coefficients model (AIOMFAC) for the medium-range and long-range interactions (interactions between solvent species and ionic species) (Zuend et al., 2011, 2010, 2008; Zuend and Seinfeld, 2012). These structure activity relationship models include parameterizations to calculate activity coefficients of aerosol mixtures containing water, several organic functional groups (e.g. carboxyl, hydroxyl aldehyde, aromatic carbon …) and inorganic ions. Since NO_2 functional group parameters were not defined in the AIOMFAC model, the parameters for alkanes were used instead. The effect of pH on phthalic acid partitioning was taken into account in SOAP based on the acid dissociation constants (pKa1=2.9, pKa2=5.5, Bang et al., 2011).

P_{sat} and ΔH_{vap} are required as input data for the model. To compute the hydrophilic partitioning, the value of the Henry's law constant is used. It can be either provided by the user or be computed from the saturation vapor pressure and the activity coefficient at infinite dilution.

SOAP can use either a dynamic approach or an equilibrium approach (assuming instantaneous partitioning) to compute OA formation. For computational purposes, the equilibrium approach was used here. The effect of modelling with SOAP non-ideality and non-equilibrium was studied previously (Kim et al., 2019).

In the equilibrium approach, the SOAP model is based on an iterative solver that computes at each iterations the partitioning of every compounds and the values of the different parameters (such as the activity coefficients) until the model has converged (low changes of concentrations between two iterations). The Newton– Raphson method is used to efficiently solve the system of equations.

10

3. Comparison between measurements and model results

3.1 Configuration

CHIMERE simulations have been performed at 0.06°x0.125° resolution over France. The number of vertical layers were 9 till 500 hPa. Meteorological data were taken from data of the Integrated Forecasting System (IFS) model from the European Centre for Medium-Range Weather Forecasts (ECMWF). Boundary conditions were obtained from a lower (0.25°x0.4°) resolution CHIMERE simulation performed on a domain covering Europe. Simulations have been performed from November 2014 to December 2015.

Annual anthropogenic emissions, classified by sector, were taken from the EMEP inventory (Vestreng, 2003). POA emissions are greatly underestimated due to a strong underestimation of residential wood burning emissions by a factor of 3 over Europe (between 1 and 10 depending on the countries) because emissions of the condensable fraction is often not considered (Denier van der Gon et al., 2015). To correct this underestimation, POA emissions were adjusted by applying an emission correction factor taken from the TNO inventory as in Couvidat and Bessagnet (2021).

In CHIMERE 2017β, POA are assumed to be semivolatile and the POA emissions are split into several SVOC with different volatilities according to the same parametrization for most of the sources (Robinson et al., 2007), except for biomass burning emissions, which are treated following the dilution curve of POA (May et al., 2013) . POA are split as described by Couvidat et al. (2012), three compounds: POAlP ($K_p = 1.1 \ m^3 \ \mu g^{-1}$), POAmP ($K_p = 0.0116 \ m^3 \ \mu g^{-1}$) and POAhP ($K_p = 0.00031 \ m^3 \ \mu g^{-1}$) having respectively a low, medium and high volatility to follow the dilution curve of POA in Robinson et al. (2007). Similarly, BOA are split into three compounds: BOAlP ($K_p = 18.3 \ m^3 \ \mu g^{-1}$), BOAmP ($K_p = 0.04 \ m^3 \ \mu g^{-1}$) and BOAhP ($K_p =$

0.00023 m^3 μg^{-1}) having respectively a low, medium and high volatility to follow the dilution curve of BOA in May et al. (2013). The aging of these compounds is also taken into account with a reaction with OH which leads to less volatile compounds (SOAlP, SOAmP and SOAhP, BSOAlP, BOAmP, BSOAhP, Kp are increased by a factor 100). The speciation of $PM_{2.5}$ emissions into POA is shown in Table S6.

For simplification purposes, and due to the lack of information on POA molecular composition, a default "average" structure representative of atmospheric POA has been assigned to these primary SVOC surrogates to calculate their activity coefficients. This default structure is composed by 40% of $C_{23}H_{47}COOH$, 5% of $C_8H_{17}CH = CHC_7H_{14}COOH$, 15% of 4-(2-propio)-syringone, 12% of $C_{29}H_{60}$ and 28% of 2-carboxybenzoic acid (EPRI, 1999).

3.2 Determination of marker precursor emissions

Since some key precursors for biomass burning aerosols, notably the non-traditional VOCs (NTVOCs) (Chrit et al., 2018), were missing among the data used for the speciation of the emissions in the CHIMERE preprocessor for the emission inventories (Passant, 2002), an update of the speciation has been performed (Table 2). Non-industrial combustion plant emissions (mainly biomass burning from domestic heating) have been especially updated in this study.

Table 2. Marker precursor percentages in non-methane hydrocarbon VOC (NMVOC) emissions from the different sectors considered.

SNAP*	BENZENE	CRESOL	GUAIACOL	NAPHTHALENE	PHENOL	TOLUENE
Combustion in energy and transformation industries	1.60[a]					1.10[a]
Non-industrial combustion plants (domestic heating)	3.16[b]	2.27[b]	1.60[b]	0.20[d]	2.85[b]	1.31[b]
Combustion in manufacturing industry	12.70[a]			0.20[a]		2.00[a]
Extraction and distribution of fossil fuels and	0.80[a]				0.20[a]	1.10[a]

geothermal energy		
Solvents and other product use	0.40 [a]	0.20 [a]
Road transport	2.54 [a]	5.20 [a]
Other mobile sources and machinery	3.00 [a]	5.21 [a]
Waste treatment and disposal	0.30 [a]	4.70 [a]
Agriculture		1.10 [a]

[*]Selected Nomenclature for reporting of Air Pollutants.
[a](Passant, 2002).
[b](Schauer et al., 2001).
[c](McDonald et al., 2000).
[d](Nalin et al., 2016).

Emission speciation was taken from biomass burning experiments performed at INERIS (AFAC, 2016; CHAMPROBOIS, 2014; Nalin et al., 2016) and from the literature (Schauer et al., 2001). When available, data from INERIS experiments were preferred due to the wood species tested (beech) typically used in France for residential heating. A value of 3.23 % of levoglucosan fraction in $PM_{2.5}$ (including condensable fraction) emitted by domestic biomass burning has been estimated from these experimental data results. Biomass burning emissions in France have been simulated following the proportions of hard and soft wood (respectively 80% and 20%) suggested by an inquiry of the French Agency for the Environment and Energy Control (ADEME) on the kind of wood burnt for domestic heating (Pouet and Gautier, 2013). To do so, the weighted mean of oak and pine (respectively hard and soft wood) emission factors previously reported (Schauer et al., 2001) has been inserted in the model.

For the phenolic compounds (phenol, cresol and guaiacol), only emissions from biomass burning have been updated. Although emissions from other sectors, notably livestock (Borhan et al., 2012; Cai et al., 2011; Hobbs et al., 2004), have been reported in literature, no data suitable for a robust estimation of the emissions have been provided.

3.3 Marker GPP sensitivity tests

In order to give insights on the importance of non-ideality and the hydrophilic partitioning, simulation tests on nitroguaiacols, nitrophenols, methylnitrocatechols and phthalic acid GPP computation have been performed during February, mid-June to mid-July and October 2015. These months have been chosen as the most representative of different annual weather and emission conditions. The configurations of the sensitivity are summarized in Table 3.

In the "reference" simulation, the targeted molecular marker is both hydrophobic and hydrophilic and all the interactions with the aerosol organic and inorganic components are considered. In the "ideal" case, the targeted molecular marker is still considered hydrophobic and hydrophilic, but the interactions with the other aerosol organic components are not considered. Non-ideal and ideal tests have also been performed by considering that the marker is only hydrophilic ("Hyphi" and "Hyphi ideal" tests respectively) or only hydrophobic ("Hypho" and "Hypho ideal").

Table 3. Configurations of the different sensitivity tests for GPP computation. Condensation onto the aqueous and organic phases is computed if the markers are considered hydrophilic and hydrophobic, respectively. Markers can be considered both hydrophilic and hydrophobic (condensation on both phases is taken into account).

Simulation	Hydrophilic markers	Hydrophobic markers	Non-ideality
Reference	True	True	True
Ideal	True	True	False
Hypho	False	True	True
Hypho ideal	False	True	False
Hyphi	True	False	True
Hyphi ideal	True	False	False

3.4 Sampling sites and collection, chemical analyses and quality control/quality assurance

Measurement and sampling details have been reported previously (see references below). A brief description is proposed hereafter. Further details are available in the SM (Table S8) and
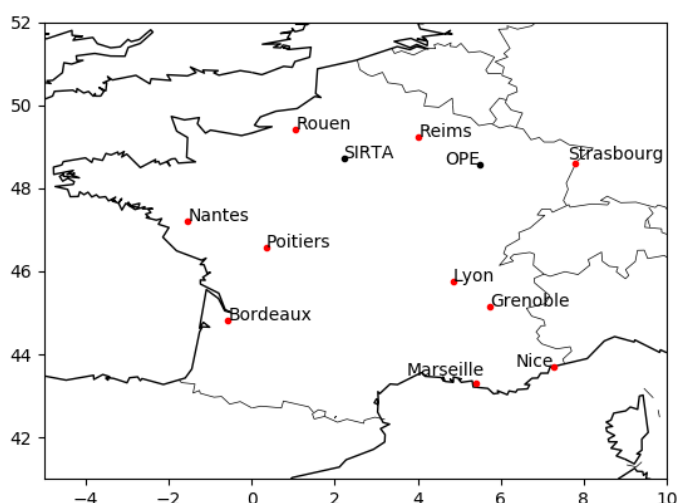
for simplification in the main text, the sites are named by the corresponding urban area, except for SIRTA and OPE. OPE is a rural site, without any village or industry within several kilometers, and so not directly influenced by anthropic activities (Golly et al., 2019, description available from http://www.andra.fr). SIRTA (Site Instrumental de Recherche par Télédétection Atmospherique, 2.15° E; 48.71° N, http://sirta.ipsl.fr) (Haeffelin et al., 2005; Zhang et al., 2019) is located approximately 25 km southwest of Paris city center and is considered as representative of the background air quality of the Ile-de-France region (Favez et al., 2021; Zhang et al., 2019).

The remaining 10 sites were of urban or sub-urban typologies, located in the main populated areas of France, and are part of the French operational network for in situ observation of PM chemical composition and sources in urban environments (CARA Program) (Favez et al., 2021).

Model results have been compared to measurements performed in the 12 different locations over France (Fig. 1). At all locations, PM_{10} samples have been collected every third or sixth days (Table S8), on pre-heated (500 °C for 12 h) quartz fiber filters (Tissu-quartz, $\emptyset$ = 150 mm, Pallflex) using high-volume samplers (30 m^3 h^{-1}, 24 h sampling, Digitel DA-80). In addition, at the SIRTA observatory gaseous phase was also collected on pre-washed polyurethane foams (PUFs, 75 mm long, PUF, Tisch Environmental, L = 75 mm, placed downstream from the filter) (Lanzafame et al., 2021). At all urban locations, sample collection has been performed during the winter 2014–2015 and over the year 2015 at SIRTA and OPE sites (Table S8). Once collected, particulate and gaseous phase samples were wrapped in aluminum foils and stored in polyethylene bags at <−18 °C until analysis. Shipping of the samples to the different laboratories for analyses have been done by express post using cool boxes (<5 °C).

The quantification of levoglucosan has been done for all sites, on the filter samples only, by IC-PAD (ion chromatography coupled to pulsed amperometric detection) (Verlhac et al., 2013; Yttri et al., 2015) while the analysis of 22 SOA markers (Table S7) has been performed on both, particulate and gaseous phases, by GC/MS (gas chromatography coupled to mass spectrometry) (Albinet et al., 2019; Lanzafame et al., 2021) at SIRTA location only. In addition, Elemental and organic carbon fractions (EC/OC) have measured on all PM samples using a Sunset lab analyzer following the EUSAAR-2 thermo-optical protocol (Cavalli et al., 2010; CEN (European Committee for Standardization), 2017).

Quality control for the quantification of SOA markers and levoglucosan has been achieved by the analysis of the NIST standard reference material SRM 1649b (urban dust). The results obtained were in good agreement with the values available in the literature for such substances not referenced in the certificate of analysis (Albinet et al., 2019; Favez et al., 2021; Verlhac et al., 2013).

Figure 1. Map showing the geographical location of the 12 sampling sites. Black points represent annual monitoring sampling sites, red points winter-time sampling campaigns.
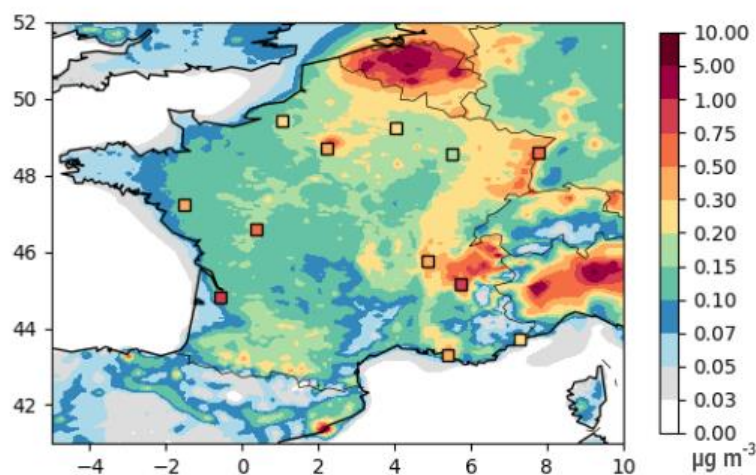
Urban and suburban sites are labelled by the agglomeration names, except for SIRTA (25 km SW of Paris). OPE is a rural site.

4. Results and discussion

4.1   Model to measurements comparison

4.1.1   Levoglucosan

Fig. 2 shows the daily modelled mean concentrations of particulate phase levoglucosan during February 2015. The sampling sites are indicated by squares filled with the mean of levoglucosan measurements performed every 3 to 6 days (sampling frequency is reported in Table S8). February is the month in which higher concentrations of levoglucosan have been observed at SIRTA during 2015. While it seems that the spatial distribution of concentrations may be well represented in the North of France and the southeastern cities, concentrations are strongly underestimated in Western France and in Mediterranean cities.

Figure 2. Average particulate phase levoglucosan concentrations (μg m^{-3}) simulated over France in February 2015. Sampling sites are highlighted by squares filled according to the average monthly concentration observed.

The underestimation of concentrations for the city of Bordeaux and over the other western cities could be due to a strong underestimation of the emissions over this area. For Nice and Marseille, part of the underestimation could be due to the low resolution of the model and the proximity to the sea (respectively ~1.75 and ~3.15 km).

Concentrations in the particle phase may be strongly affected by GPP. Modelled particulate phase levoglucosan fraction spatial distributions and mean values for each city are reported and commented in the SM (section 3.1, Fig. S6 and Table S9). Whereas levoglucosan used to be considered as almost non-volatile (Fraser and Lakshmanan, 2000; Locker, 1988; Simoneit et al., 1999), recent studies demonstrated the presence of levoglucosan in the gaseous phase in ambient air conditions (Hennigan et al., 2010; May et al., 2012a; Pratap et al., 2019; Xie et al., 2014). In agreement the results reported by Pratap et al. (2019), our model estimates that 20 to 100% of levoglucosan is associated to the particle phase. However, the highest incertitude in this GPP parametrization is associated to the saturated vapor pressure and vaporization enthalpy choice. In this study, the saturation vapor pressure value measured by Booth et al., (2011) was used, which is relatively high (1.45×10^{-6} torr). To our knowledge, no other measurements of levoglucosan P_{sat} have been performed. Xie et al., (2014) performed computation of the levoglucosan partitioning but with a much lower saturation vapor pressure (1.8×10^{-7} torr against 1.45×10^{-6} torr for the value used in this study) and higher vaporization enthalpy. This lower saturation vapor pressure was taken from Parshintsev et al., (2011) who did not explain how this value was estimated. Similarly, using the Psat from Parshintsev et al.
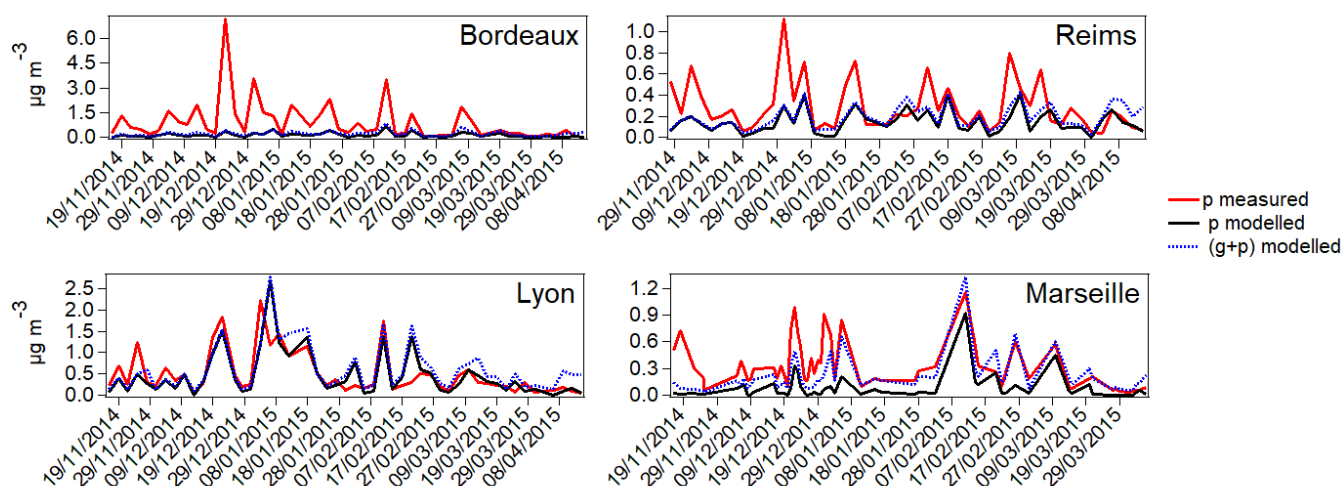
(2011), Li et al. (2021) estimated that less than 7% of levoglucosan would be present in the gas-phase. It may therefore be possible that the value used in the present study is overestimated. Using the value from Parshintsev et al. (2011) would lead to a significant increase of the particle-phase levoglucosan that would almost appear as non-volatile.

In Fig. 3, the temporal variations of measured and modelled particulate phase levoglucosan, together with the modelled total (gaseous + particulate phases) concentrations are reported for Bordeaux, Reims, Lyon and Marseille. These sites have been selected as they are representative of the different geographical distribution (Northern, Western, South-eastern and Mediterranean cities). For the other winter sites (Rouen, Strasbourg, Nantes, Poitiers, Grenoble and Nice) the comparisons are reported in Fig. S7. Annual levoglucosan variations are reported in Fig. 4 for SIRTA and in Fig. S8 for OPE.

For most of the cities the measured temporal trends were well reproduced (correlations between 0.67 and 0.75) except for Rouen and Nice (correlations of 0.38 and 0.35 respectively). However, concentrations are strongly underestimated for the western and northern cities (MNB between -38% and -78%). The concentrations in the southern Mediterranean cities (Marseille and Nice) were also strongly underestimated (MNBs are -79% and 75% respectively) but, contrary to the Northern and Western cities, this underestimation could be attributed to an underestimation of the GPP as the order of magnitude was well represented by the model when the gaseous phase concentration was included (MNBs of -15% and -7% respectively). The order of magnitude of modelled concentration was in good agreement with measurements for southeastern cities (Lyon and Grenoble, MNBs of 10% and 12% respectively). At SIRTA, Fig. 4, the modelled levoglucosan concentrations matched well with the lower concentrations in the first part of the year but did not reach the concentration of

the major peak observed the 13/02. Modelled levoglucosan at OPE had the same magnitude order and similar temporal variations than the measured levoglucosan.

Overall, a similar bias was often obtained between OM and levoglucosan concentrations in winter. The comparisons of measured and modelled OM temporal variation are shown in the Fig. 4 for SIRTA and in the SM for other stations (Fig. S9 for Bordeaux, Reims, Lyon, Marseille, Rouen, Strasbourg, Nantes, Poitiers, Grenoble and Nice, data not provided for OPE). In western and northern cities, the similar significant underestimation between OM (MNBs between –0.49 and -0.67) and levoglucosan concentrations suggests that the underestimation of the biomass burning emissions over these areas could be a likely explanation. The different performances observed for levoglucosan and OM simulation for the other winter stations suggested that other factors (GPP, degradation, etc…) could significantly affect levoglucosan modelling. At SIRTA, from January to the beginning of May, the model manages to reproduce both the concentrations of OM and levoglucosan indicating a good representation of biomass burning emissions during this period. The opposite behavior is observed in fall (in December 2014 and from October to December 2015) as both the concentrations of OM and levoglucosan are strongly underestimated. This feature could be explained by an underestimation of biomass burning emissions during this period.

Figure 3. Model to measurements comparison of levoglucosan concentrations in 4 urban sites (Bordeaux, Reims, Lyon and Marseille) in France during the winter 2014/2015.

4.1.2 Nitroguaiacols and nitrophenols

Simulated nitroguaiacols total concentrations are compared to 4-nitroguaiacol measured concentrations (Fig. 4). As mentioned in section 2.1, it is not possible to estimate the 4-nitroguaicol percentage on the total nitroguaiacol concentration inducing that an underestimation by the model can be expected.

Nitroguaiacols concentrations were stimulated with the right order of magnitude. The modelled higher concentrations (average of 25.8 ng m^{-3}) at the beginning of the year (January to March) agreed well with the observations (average of 20.8 ng m^{-3}), while in April–May the model (average of 14 ng m^{-3}) overestimated the measurements (average of 1.5 ng m^{-3}). In summer, nitroguaiacol concentrations were very low in both model and measurements (under 6 and 1 ng m^{-3} respectively). The weak increase of concentrations observed at the end of the year has been well reproduced by the model.

Nitrophenols (2- and 4- nitrophenol sum) concentrations were well simulated for most of the year. The model succeeded to capture the high concentrations observed from January to April and the strong decrease of concentrations during summer. Concentrations from February to April were however overestimated. At the end of the year, the model underestimated the concentrations by a factor 11 and was not able to reproduce the peaks observed.

The underestimation of nitrophenol concentrations during winter is likely related to a lack of biomass burning emissions, confirmed by the strong underestimation of levoglucosan concentrations during the same period. Moreover, while the model considers that toluene, benzene and phenol are nitrophenol precursors, other precursors could be missing from the model. Nitrophenols primary emission during biomass burning episodes have been recently observed (Salvador et al., 2020) and should be also added to the model.

The percentage of nitrophenols produced by toluene oxidation in February has been determined to be less than 1%, while primary phenol accounted for 40% of nitrophenols production, and benzene for the remaining fraction. Therefore, benzene was the most important precursor for nitrophenols in our model.

The overestimation of nitrophenols concentrations from February to April do not follow the same pattern than levoglucosan that was underestimated for this period. This difference could be related to an overestimation of the chemical formation during this period (due to nitration of phenols for example) or missing removal processes (for example lack of deposition or chemical destruction).4.1.3 Methylnitrocatechols

Methylnitrocatechols (sum of 3-methyl-5-nitrocatechol, 4-methyl-5-nitrocatechol and 3-methyl-6-nitrocatechol) were underestimated by the model by a factor 60 during the cold

season (January–April and September–December) and by a factor 4 in the warmest season (May–August) (Fig. 4). In winter, methylnitrocatechols measured concentrations were higher and their temporal evolution was well reproduced. During spring–summer, measured methylnitrocatechols was very low, while the model simulated a strong increase of concentrations in April–May and multiple small peaks in the rest of the period.
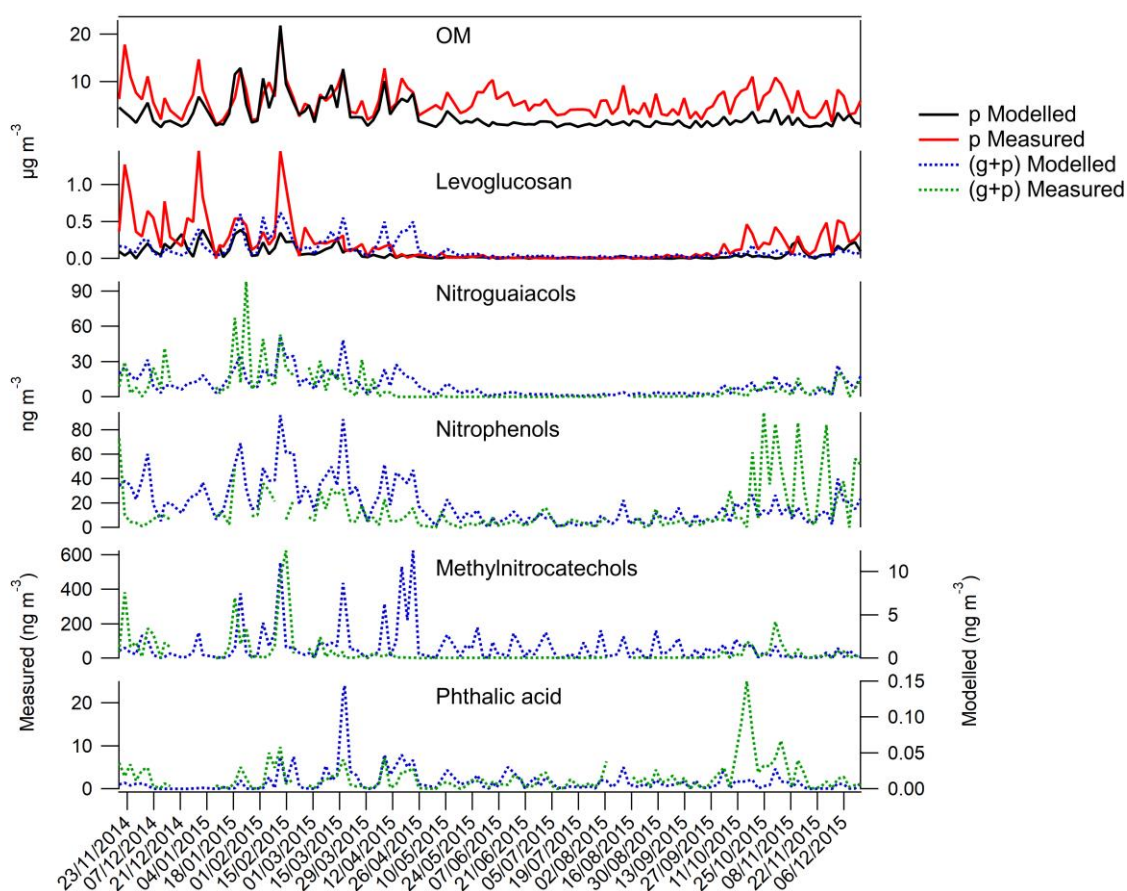
The performances of the model in reproducing methylnitrocatechols temporal variations depended on the seasonal contribution of the different emission sectors. In winter, biomass burning was expected to be the main contributor, while in summer the sum of other emission sector (such us vehicular) contributions was higher. Measured methylnitrocatechols and levoglucosan correlated well (r=0.70, p<0.05), demonstrating that methylnitrocatechol was a good marker for biomass burning SOA in the atmosphere. However, the correlation between these two compounds in the model (r=0.2, p<0.05) was scarce, indicating that a significant contribution from biomass burning was probably missing for methylnitrocatechols. Based on these results, we can assert that biomass burning methylnitrocatechols was probably strongly underestimated.

A possible reason for the underestimation of methylnitrocatechols could be missing sources. For example, Hobbs et al., (2004) estimated that 19% of NMVOC emission from Livestock in UK could be cresol. Based on the amount of cresol in residential wood burning emissions (Table 2) and by using emission estimates from the EMEP inventory, emissions from Livestock could therefore account for 20 times more cresol than residential wood burning. These emissions would not explain the high concentrations in winter that seem to indicate a high contribution from biomass burning. However, livestock emissions (or emissions from other sources) could explain the low concentrations of methylnitrocatechols observed in summer.

23

Moreover, in our model methylcatechol has been considered exclusively as an intermediate, while it has been measured in primary biomass burning emissions (Gonçalves et al., 2012; Hatch et al., 2018). According to the data of Gonçalves et al. (2012), methylcatechol could represent (depending on the heating device) between 3% and 14% of the levoglucosan emissions. The potential primary methylcatechol contribution to methylnitrocatechol concentrations has been estimated by adding to methylcatechol emissions (chosen as 10% of the levoglucosan emissions). Methylnitrocatechols concentrations may increase by a factor 10, demonstrating that methylcatechol contribution to methylnitrocatechols total concentrations may be significant and could explain part of the discrepancy between the model and measurements.

Wang et al. (2017) measured methylnitrocatechols primary emissions from biomass burning sources. Based on this study, it only accounts for a small fraction of the $PM_{2.5}$ emissions (between 0.0001% and 0.07%). For a concentration of biomass burning OA of 10 µg m^{-3}, primary methylnitrocatechol concentrations would be at most around 7 ng m^{-3}. In the current state of knowledge, it is difficult to definitively conclude on the reasons for these underestimations.

Figure 4. Annual evolution of OM, levoglucosan, nitroguaiacol, nitrophenols, methylnitrocatechols and phthalic acid concentrations at SIRTA, 2015.

4.1.3   Phthalic acid

Phthalic acid model to measurements comparison is presented in Fig. 4. The measured phthalic acid concentrations are below 25 ng m^{-3}, with higher concentrations observed between mid-October and the beginning of November. The simulated concentrations of phthalic acid are two order of magnitude lower than the observations and the temporal variations are also misrepresented.

To verify whether the mechanism parametrization could explain the underestimation of phthalic acid formation, a simpler mechanism based on observed experimental yields has

been developed. By combining the two-product Odum parameterization for Naphthalene SOA of Chan et al. (2009) to the data of Kleindienst et al. (2012) on phthalic acid to SOA ratio, phthalic acid molar yields of 1.8% and 4.7% have been determined respectively under high-NO_x and low-NO_x conditions (a molar yield around 5% can be estimated with the extended mechanism when all reactions up to the formation of phthalic acid are considered). These yields would correspond to molar fractions of 6.9% and 10.7% of H^2O surrogates AnPAHhN and AnPAHlN (Couvidat et al., 2013b), the SOA surrogates for naphthalene SOA based on Chan et al. (2009). The amount of phthalic acid estimated by this methodology is in the same order of magnitude than the amount simulated with the extended mechanism. The concentration ratios between the simple mechanism and the extended mechanism are between a factor 0.5 to 5 with a factor close to 1 for most of France except for areas with high emissions. At SIRTA, a ratio of 1.6 was determined. The higher concentrations over the high emission areas with the simpler mechanism can be explained by the number of chemical steps in the mechanism (the yield-based parameterization for phthalic acid formation is a single-step process contrary to the extended mechanism), showing the importance of a detailed mechanism to simulate SOAformation.

Since both methods (based on theory and on experimental yields) fail in estimating measured phthalic acid concentrations, it seems unlikely that the concentrations of phthalic acid in ambient air can be explained by the oxidation of naphthalene alone. Other gaseous polycyclic aromatic hydrocarbons (PAH) could contribute to the formation but naphthalene dominates the emissions of gaseous PAH (McDonald et al., 2000, Schauer et al., 2001).

Other phthalic acid sources should be considered to explain the discrepancies observed. Recent studies assess that phthalates concentrations are very high in urban environment (Barreca et al., 2014; He et al., 2018; Simoneit et al., 2005; Teil et al., 2006) and their

degradation in atmosphere can produce phthalic acid (Hankett et al., 2013). In the Paris urban area phthalate esters atmospheric levels have been evaluated to be around 55 ng m^{-3} (Teil et al., 2006). Phthalate esters could be significant precursors of phthalic acid in the atmosphere, but not enough information has been provided in the literature to quantify their contribution to total phthalic acid concentrations. Moreover, phthalic acid has been also quantified in primary vehicular emissions (Kawamura and Kaplan, 1987).

4.2   GPP estimations: secondary markers at SIRTA

The results on GPP estimations according to the different parametrization tests performed are shown in Fig. 5, together with the results of measurements ("obs") and of the reference simulation GPP.

All the molecular markers in the only "hydrophilic" test partitioned similarly to the "reference" simulation. This indicates that the partitioning of the markers are dominated by the hydrophylic partitioning (condensation onto the aqueous phase of particles). Slight differences between the "reference" and the "hydrophilic" tests (~5% both in median and interquartile range of the particulate fraction, F_p) and between the "ideal" and "hydrophilic ideal" tests (~18% for the median and interquartile range F_p) have been found for all the molecular markers. On the contrary, the hydrophobic partitioning of molecular markers in non-ideal aerosol was close to zero for all the markers, with no variability indicating that none of the studied compounds could be considered as strongly hydrophobic.
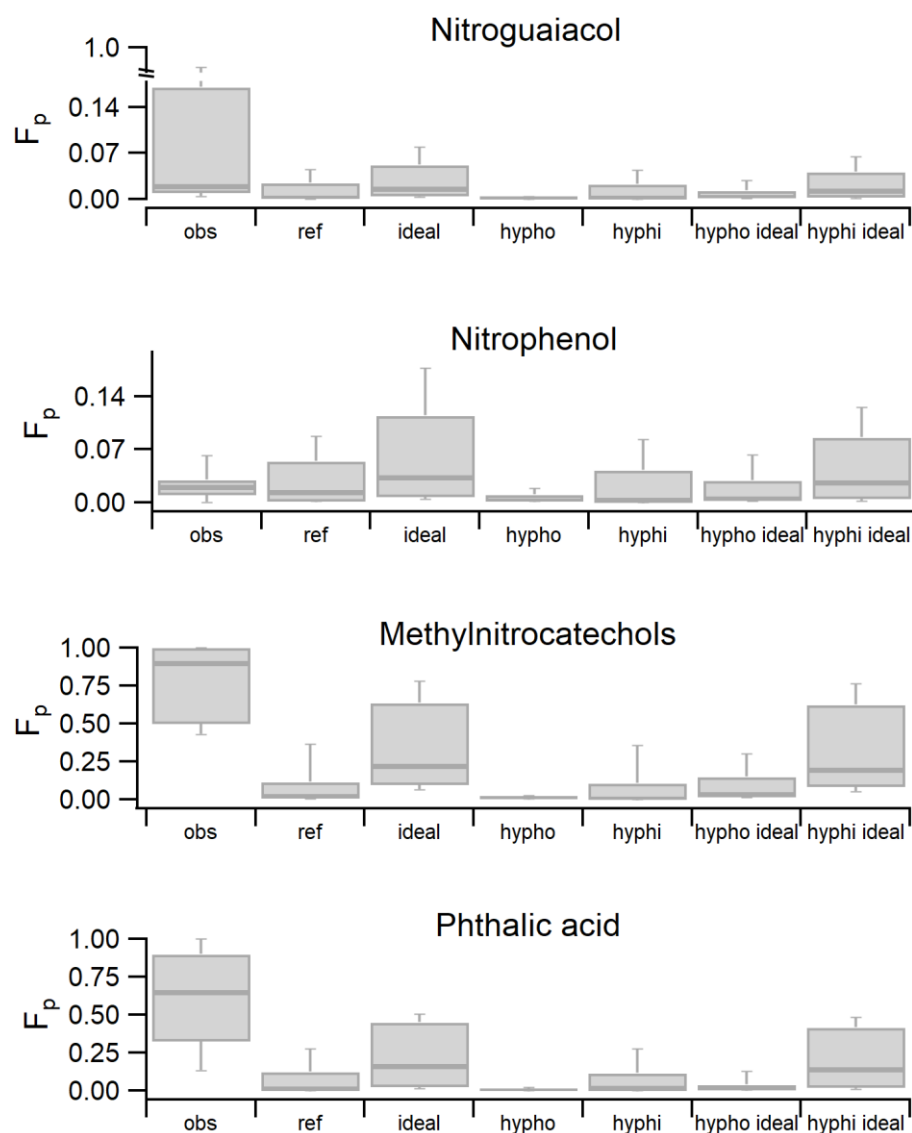
Measurement results showed that nitroguaiacol and nitrophenol are mostly in the gaseous phase with measured medians F_p lower than 5%. In all the simulation tests performed, the particulate phase fraction remains very low and the median value never exceeds 5%. While Fp

is low for both the model results and measurements, the model tends to underestimate Fp. However, "Ideal" nitroguaiacol median F_p (0.015) is closer to the observed one (0.02) than the "reference" (0.002). In that case, considering the influence of non-ideality lead to a decrease of F_p and to an underestimation of the particle-phase fraction.

Methylnitrocatechols and phthalic acid GPP is shifted towards the particulate phase in the measurements (median F_p of 0.9 0.65 respectively) whereas, in all the model runs, they are mainly present in the gas phase (median F_p ranges between 0.02 and 0.25) and their F_p are strongly underestimated.

In general, we can assert that the GPP of the molecular markers is driven mainly by their hydrophilicity and that the model tends to underestimate the particle phase fraction. Molecular marker partitioning in the "ideal" simulations was found to be closer to the measurements because in the "ideal" simulations the particle phase fraction is higher. These considerations should be taken carefully because of the approximations used in the model. Some functional groups, or the combination of functional groups, could be not well represented in the SAR used to estimate the activity coefficients (e.g. the NO_2 group). The saturation vapor pressure used in this study are as well highly uncertain, modelled OM is strongly underestimated in summer and OM composition could be not representative of real OM since an apolar default structure is used for primary compounds, and the model could strongly underestimate the concentrations of hydrophilic aerosols. Moreover, the equilibrium assumption could be a reason of underestimation. Kim et al., (2019) simulated the influence of particle viscosity on hydrophobic compounds GPP using a dynamic approach. In a dynamic inviscid approach, particulate phase concentrations are close to equilibrium, while in a dynamic viscous approach hydrophobic SOA concentrations increase significantly for volatile

compounds and deviate significantly from equilibrium. This deviation from equilibrium could therefore be a reason for the underestimation of the GPP in our study.

Figure 5. Comparison between the observed and modelled particulate fractions (F_p) according to the different parametrization tests performed. From the top to the bottom: nitroguaiacol, nitrophenol, methylnitrocatechols and phthalic acid gas/particle partitioning thermodynamic

tests. On the right side, the particulate phase fractions calculated for measurements (obs) and simulated with reference (ref), ideal aerosol (ideal), hydrophobic marker (hypho), hydrophilic marker (hyphi), hydrophobic marker and ideal aerosol (hypho ideal) and hydrophilic marker and ideal aerosol (hyphi ideal) parameterizations are shown.

4.3 Evaluation of the OA-tracer approach to evaluate the wood-burning OM

Constant ratios between OM_{wb} and particulate phase levoglucosan (pLEVO) are often used to evaluate the contribution of wood-burning aerosol to organic aerosol (Herich et al., 2014; Puxbaum et al., 2007; Schmidl et al., 2008). However, the partitioning of levoglucosan may depend strongly on the hydrophilic properties, on the environmental conditions and on non-ideality. Moreover, the partitioning of levoglucosan probably differs from the partitioning of wood burning SVOC. The OM_{wb}/pLEVO could therefore depend on environmental conditions. The simulated OM_{wb}/pLEVO over France as a function of total OM at 275, 280 and 285 ($\pm$ 0.5) K are reported in Fig. 6 for the reference simulations as well as the ideal and the hydrophobic ideal test (by considering all the data points of the domain close to the selected temperature $\pm$ 0.5 K). The ratio has been calculated for levoglucosan concentrations greater than 0.1 μg m^{-3}. The selected temperatures have been chosen to be representative of wintertime, during which OM_{wb} and levoglucosan emissions are expected to be higher.
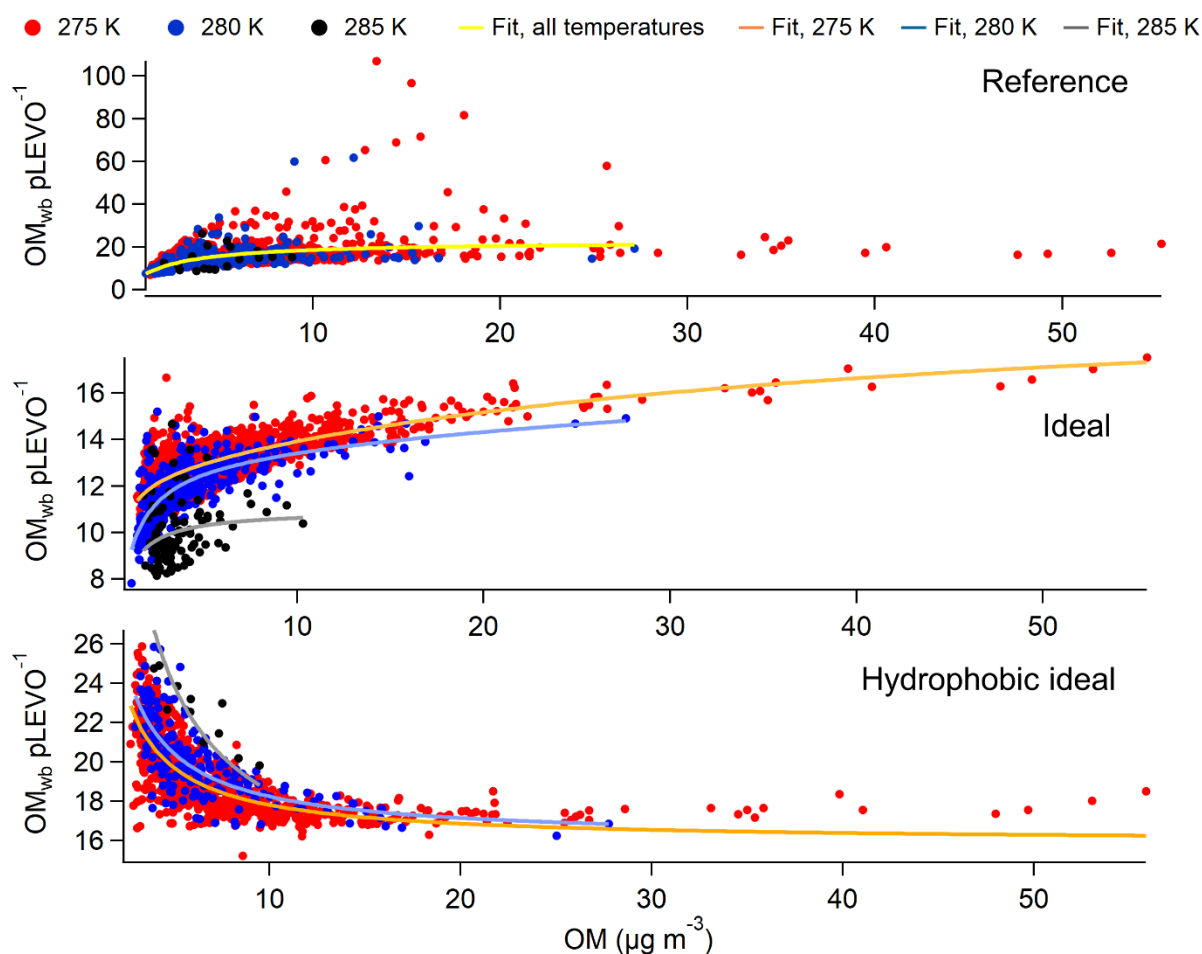
All the tests indicate strong variations of the OM_{wb}/pLEVO. The ratio varies strongly under 10 μg m^{-3} of OM while above 10 μg m^{-3} simulation results indicate low variation of this ratio. Whatever the temperature regime, at OM values below 10 μg m^{-3}, the constant ratio approach commonly used to calculate OM_{wb} cannot be validated because of the great variability. It can therefore be difficult to evaluate precisely the contribution of OM_{wb} from levoglucosan alone.

However, the use of constant ratios to apportion OM_{wb} from levoglucosan concentrations could be considered accurate during winter pollution episodes characterized by high OM concentration above 10 µg m^{-3}, most of the ratio values are around 20.

The computation of the ratio could be affected by differences in performance for levoglucosan and biomass burning SVOC partitioning. The partitioning of levoglucosan was not evaluated as measurement of gas-phase concentrations of levoglucosan were not available. It could therefore be necessary to design specific experiments to validate the previous conclusions and capacity of the model to reproduce OM_{wb}/pLEVO ratios.

The computation of the ratio is affected by the assumptions on the GPP (ideal hydrophilic partitioning, ideal hydrophobic partitioning or non-ideal partitioning on both phases). In the hydrophobic ideal test, the ratio decreases fast for OM values below 10 µg m^{-3} (from 26 to 18) and at higher OM masses keeps a value around 18, following an inverse Odum-like curve indicating that $SVOC_{wb}$ GPP grow faster than levoglucosan GPP when OM is increasing. In the ideal test (which also considers the hydrophilic partitioning), the OM_{wb}/pLEVO ratio varies between 8 and 16 and follows an Odum-like curve. This trend is determined by the relative variations of levoglucosan and OM_{wb} volatilities: levoglucosan appears non-volatile when the ideal hydrophilic partitioning is accounted for (as shown in section 4.2.1) and its partitioning does not depend on OM while the condensation of $SVOC_{wb}$ increase with OM (and follow the dilution curve of May et al., (2012b)). When non-ideality is considered, strong variability of this ratio is simulated, especially under 10 µg m^{-3} where the ratio varied in the simulations between 6 and 40.

Figure 6. Odum-like curves representing OM_{wb} $pLEVO^{-1}$ as a function of total OM at 275, 280 and 285 K. From the top to the bottom: 1. Reference run, with a single Odum-like theoretical curve to represent the variation at all the selected temperatures; 2. Ideal run, for which 3 Odum-like theoretical curves have been calculated; 3. Hydrophobic ideal aerosol run, that follows a temperature dependent inverse Odum parametrization. All the regression lines have been calculated with a non-linear least-squares data fitting method.

Conclusions

A mechanism for the formation of molecular markers has been implemented in the 3D chemistry transport model CHIMERE.

Levoglucosan concentration is reproduced by the model with the same performances as OM.

An underestimation of the residential wood burning emissions for some cities in France is probably the cause of the mismatching between measurements and simulation outputs.

Nitroguaiacol and nitrophenol concentrations are well simulated by the model, while methylnitrocatechol and phthalic acid are strongly underestimated, and their temporal variations are not consistent with the measurements. The analysis seems to underline missing precursor sources (for example livestock), an underestimation of precursor emissions, missing precursors (e.g. methylcatechol for methylnitrocatechol), non-accounted primary marker emissions (methylnitrocatechols and phthalic acid have been detected in emissions) or missing chemical pathways. Precursor emissions probably contribute largely to the simulation uncertainties for these compounds. The results of this study may indicate that anthropogenic SOA is formed from a greater variability of sources and precursors than currently considered in air quality models. Therefore, the molecular approach seems convenient to achieve a better knowledge of anthropogenic aerosol sources, which may provide a valuable contribution to a better understanding of the complex links between climate change and air pollution.

The GPP of the different molecular markers has been simulated with SOAP by considering non-ideality. For nitroguaiacol and nitrophenols the model reproduces well the GPP, but in general the model underestimates the measured marker F_p, especially when only the ideal partitioning on the organic phase is considered, which is the current assumption of most air quality models. For all the markers, the GPP seems to be dominated by the hydrophilic partitioning. The gas to particle partitioning may therefore be a key issue in SOA modelling and further investigations are probably needed to evaluate the ability of CTM to reproduce GPP. For levoglucosan, different studies reported different values of the saturation vapor pressure. The choice of the saturation vapor pressure could be critical and depending on the value, levoglucosan could appear as semi-volatile or as almost non-volatile.

A theoretical study of the OM/pLEVO ratio demonstrates that levoglucosan contribution to OM_{wb} is not constant at OM values typical of European aerosol (<10 µg m^{-3}) contrary to what

is assumed in numerous studies using this marker for source apportionment. For higher OM concentrations, observed during intense winter pollution episodes, the model seems to indicate that this ratio can be assumed as constant.

Our results show that marker modelling can give insights on some processes (such as precursor emissions or missing mechanisms) involved in SOA formation and could be used to evaluate the GPP in 3D air quality models. Although challenging (in regard to the uncertainty on emissions, chemical mechanism and thermodynamic parameters), marker modelling proves to be valuable to understand SOA formation and helpful to fill the gap between model and measurements.

Acknowledgments

References

AFAC, 2016. Détermination de facteurs d'émission de polluants des foyers domestiques alimentés au bois (No. 1362C0002). ADEME.

Albinet, A., Lanzafame, G.M., Srivastava, D., Bonnaire, N., Nalin, F., Wise, S.A., 2019. Analysis and determination of secondary organic aerosol (SOA) tracers (markers) in particulate matter standard reference material (SRM 1649b, urban dust). Anal Bioanal Chem. https://doi.org/10.1007/s00216-019-02015-6

Al Naiema, I.M., Offenberg, J.H., Madler, C.J., Lewandowski, M., Kettler, J., Fang, T., Stone, E.A., 2020. Secondary organic aerosols from aromatic hydrocarbons and their contribution to fine particulate matter in Atlanta, Georgia. Atmospheric Environment 223, 117227. https://doi.org/10.1016/j.atmosenv.2019.117227

Al Naiema, I.M., Stone, E.A., 2017. Evaluation of anthropogenic secondary organic aerosol tracers from aromatic hydrocarbons. Atmospheric Chemistry and Physics 17, 2053–2065. https://doi.org/10.5194/acp-17-2053-2017

Bannan, T.J., Booth, A.M., Jones, B.T., O'Meara, S., Barley, M.H., Riipinen, I., Percival, C.J., Topping, D., 2017. Measured Saturation Vapor Pressures of Phenolic and Nitro-aromatic Compounds. Environmental Science & Technology 51, 3922–3928. https://doi.org/10.1021/acs.est.6b06364

Barreca, S., Indelicato, R., Orecchio, S., Pace, A., 2014. Photodegradation of selected phthalates on mural painting surfaces under UV light irradiation. Microchemical Journal 114, 192–196. https://doi.org/10.1016/j.microc.2014.01.004

Bessagnet, B., Pirovano, G., Mircea, M., Cuvelier, C., Aulinger, A., Calori, G., Ciarelli, G., Manders, A., Stern, R., Tsyro, S., García Vivanco, M., Thunis, P., Pay, M.-T., Colette, A., Couvidat, F., Meleux, F., Rouïl, L., Ung, A., Aksoyoglu, S., Baldasano, J.M., Bieser, J., Briganti, G., Cappelletti, A., D&apos;Isidoro, M., Finardi, S., Kranenburg, R., Silibello, C., Carnevale, C., Aas, W., Dupont, J.-C., Fagerli, H., Gonzalez, L., Menut, L., Prévôt, A.S.H., Roberts, P., White, L., 2016. Presentation of the EURODELTA III intercomparison exercise – evaluation of the chemistry transport models' performance on criteria pollutants and joint analysis with meteorology. Atmospheric Chemistry and Physics 16, 12667–12701. https://doi.org/10.5194/acp-16-12667-2016

Bey, I., Jacob, D.J., Yantosca, R.M., Logan, J.A., Field, B.D., Fiore, A.M., Li, Q., Liu, H.Y., Mickley, L.J., Schultz, M.G., 2001. Global modeling of tropospheric chemistry with assimilated meteorology: Model description and evaluation. Journal of Geophysical Research: Atmospheres 106, 23073–23095. https://doi.org/10.1029/2001JD000807

Bhattarai, H., Saikawa, E., Wan, X., Zhu, H., Ram, K., Gao, S., Kang, S., Zhang, Q., Zhang, Y., Wu, G., Wang, X., Kawamura, K., Fu, P., Cong, Z., 2019. Levoglucosan as a tracer of biomass burning: Recent progress and perspectives. Atmospheric Research 220, 20–33. https://doi.org/10.1016/j.atmosres.2019.01.004

Bilde, M., Barsanti, K., Booth, M., Cappa, C.D., Donahue, N.M., Emanuelsson, E.U., McFiggans, G., Krieger, U.K., Marcolli, C., Topping, D., Ziemann, P., Barley, M., Clegg, S., Dennis-Smither, B., Hallquist, M., Hallquist, Å.M., Khlystov, A., Kulmala, M., Mogensen, D., Percival, C.J., Pope, F., Reid, J.P., Ribeiro da Silva, M.A.V., Rosenoern, T., Salo, K.,

Soonsin, V.P., Yli-Juuti, T., Prisle, N.L., Pagels, J., Rarey, J., Zardini, A.A., Riipinen, I., 2015. Saturation Vapor Pressures and Transition Enthalpies of Low-Volatility Organic Molecules of Atmospheric Relevance: From Dicarboxylic Acids to Complex Mixtures. Chemical Reviews 115, 4115–4156. https://doi.org/10.1021/cr5005502

Booth, A.M., Bannan, T., McGillen, M.R., Barley, M.H., Topping, D.O., McFiggans, G., Percival, C.J., 2012. The role of ortho, meta, para isomerism in measured solid state and derived sub-cooled liquid vapour pressures of substituted benzoic acids. RSC Advances 2, 4430. https://doi.org/10.1039/c2ra01004f

Booth, A.M., Montague, W.J., Barley, M.H., Topping, D.O., McFiggans, G., Garforth, A., Percival, C.J., 2011. Solid state and sub-cooled liquid vapour pressures of cyclic aliphatic dicarboxylic acids. Atmospheric Chemistry and Physics 11, 655–665. https://doi.org/10.5194/acp-11-655-2011

Borhan, M.S., Capareda, S., Mukhtar, S., Faulkner, W.B., McGee, R., Jr, C.B.P., 2012. Comparison of seasonal phenol and p-cresol emissions from ground-level area sources in a dairy operation in central Texas. Journal of the Air & Waste Management Association 62, 381–392. https://doi.org/10.1080/10473289.2011.646050

Bressi, M., Cavalli, F., Putaud, J.P., Fröhlich, R., Petit, J.-E., Aas, W., Äijälä, M., Alastuey, A., Allan, J.D., Aurela, M., Berico, M., Bougiatioti, A., Bukowiecki, N., Canonaco, F., Crenn, V., Dusanter, S., Ehn, M., Elsasser, M., Flentje, H., Graf, P., Green, D.C., Heikkinen, L., Hermann, H., Holzinger, R., Hueglin, C., Keernik, H., Kiendler-Scharr, A., Kubelová, L., Lunder, C., Maasikmets, M., Makeš, O., Malaguti, A., Mihalopoulos, N., Nicolas, J.B., O'Dowd, C., Ovadnevaite, J., Petralia, E., Poulain, L., Priestman, M., Riffault, V., Ripoll, A., Schlag, P., Schwarz, J., Sciare, J., Slowik, J., Sosedova, Y., Stavroulas, I., Teinemaa, E., Via, M., Vodička, P., Williams, P.I., Wiedensohler, A., Young, D.E., Zhang, S., Favez, O., Minguillón, M.C., Prevot, A.S.H., 2021. A European aerosol phenomenology - 7: High-time resolution chemical characteristics of submicron particulate matter across Europe. Atmospheric Environment: X 10, 100108. https://doi.org/10.1016/j.aeaoa.2021.100108

Byun, D., Schere, K.L., 2006. Review of the Governing Equations, Computational Algorithms, and Other Components of the Models-3 Community Multiscale Air Quality (CMAQ) Modeling System. Applied Mechanics Reviews 59, 51–77. https://doi.org/10.1115/1.2128636

Cai, L., Koziel, J.A., Zhang, S., 2011. Odorous chemical emissions from livestock operations in United States. IEEE Conference Publication. https://doi.org/10.1109/rsete.2011.5964331

Camredon, M., Aumont, B., Lee-Taylor, J., Madronich, S., 2007. The SOA/VOC/NO$_x$ system: an explicit model of secondary organic aerosol formation. Atmospheric Chemistry and Physics 7, 5599–5610. https://doi.org/10.5194/acp-7-5599-2007

Carlton, A.G., Wiedinmyer, C., Kroll, J.H., 2009. A review of Secondary Organic Aerosol (SOA) formation from isoprene. Atmospheric Chemistry and Physics 9, 4987–5005. https://doi.org/10.5194/acp-9-4987-2009

Cavalli, F., Viana, M., Yttri, K.E., Genberg, J., Putaud, J.-P., 2010. Toward a standardised thermal-optical protocol for measuring atmospheric organic and elemental carbon:

the EUSAAR protocol. Atmospheric Measurement Techniques 3, 79–89. https://doi.org/10.5194/amt-3-79-2010

CEN (European Comittee for Standardization), 2017. EN 16909:2017 - Ambient air - Measurement of elemental carbon (EC) and organic carbon (OC) collected on filters. CEN, Brussels (Belgium).

CHAMPROBOIS, 2014. Transformation physico-chimique d'un aerosol de combustion de bois en champ proche de la source (No. DRC-14-128277-11309A). ADEME.

Chan, A.W.H., Kautzman, K.E., Chhabra, P.S., Surratt, J.D., Chan, M.N., Crounse, J.D., Kürten, A., Wennberg, P.O., Flagan, R.C., Seinfeld, J.H., 2009. Secondary organic aerosol formation from photooxidation of naphthalene and alkylnaphthalenes: implications for oxidation of intermediate volatility organic compounds (IVOCs). Atmospheric Chemistry and Physics 9, 3049–3060

Chrit, M., Sartelet, K., Sciare, J., Pey, J., Nicolas, J.B., Marchand, N., Freney, E., Sellegri, K., Beekmann, M., Dulac, F., 2018. Aerosol sources in the western Mediterranean during summertime: a model-based approach. Atmospheric Chemistry and Physics 18, 9631–9659. https://doi.org/10.5194/acp-18-9631-2018

Coeur-Tourneur, C., Cassez, A., Wenger, J.C., 2010. Rate Coefficients for the Gas-Phase Reaction of Hydroxyl Radicals with 2-Methoxyphenol (Guaiacol) and Related Compounds. The Journal of Physical Chemistry A 114, 11645–11650. https://doi.org/10.1021/jp1071023

Couvidat, F., Bessagnet, B., 2021. Role of ecosystem-atmosphere exchanges of semi-volatile organic compounds in organic aerosol formation. Atmospheric Environment 263, 118541. https://doi.org/10.1016/j.atmosenv.2021.118541

Couvidat, F., Bessagnet, B., Garcia-Vivanco, M., Real, E., Menut, L., Colette, A., 2018. Development of an inorganic and organic aerosol model (CHIMERE 2017β v1.0): seasonal and spatial evaluation over Europe. Geoscientific Model Development 11, 165–194. https://doi.org/10.5194/gmd-11-165-2018

Couvidat, F., Debry, E., Sartelet, K., Seigneur, C., 2012. A hydrophilic/hydrophobic organic (H2O) aerosol model: Development, evaluation and sensitivity analysis. Journal of Geophysical research 117, D10304. https://doi.org/10.1029/2011JD017214

Couvidat, F., Kim, Y., Sartelet, K., Seigneur, C., Marchand, N., Sciare, J., 2013b. Modeling secondary organic aerosol in an urban area: application to Paris, France. Atmospheric Chemistry and Physics 13, 983–996. https://doi.org/10.5194/acp-13-983-2013

Couvidat, F., Sartelet, K., 2015. The Secondary Organic Aerosol Processor (SOAP v1.0) model: a unified model with different ranges of complexity based on the molecular surrogate approach. Geoscientific Model Development 8, 1111–1138. https://doi.org/10.5194/gmd-8-1111-2015

Couvidat, F., Sartelet, K., Seigneur, C., 2013a. Investigating the Impact of Aqueous-Phase Chemistry and Wet Deposition on Organic Aerosol Formation Using a Molecular Surrogate Modeling Approach. Environ. Sci. Technol. 47, 914–922. https://doi.org/10.1021/es3034318

Debry, E., Fahey, K., Sartelet, K., Sportisse, B., Tombette, M., 2007. Technical Note: A new SIze REsolved Aerosol Model (SIREAM). Atmospheric Chemistry and Physics 7, 1537–1547. https://doi.org/10.5194/acp-7-1537-2007

Denier van der Gon, H. a. C., Bergström, R., Fountoukis, C., Johansson, C., Pandis, S.N., Simpson, D., Visschedijk, A.J.H., 2015. Particulate emissions from residential wood combustion in Europe – revised estimates and an evaluation. Atmospheric Chemistry and Physics 15, 6503–6519. https://doi.org/10.5194/acp-15-6503-2015

Derognat, C., Beekmann, M., Baeumle, M., Martin, D., Schmidt, H., 2003. Effect of biogenic volatile organic compound emissions on tropospheric chemistry during the Atmospheric Pollution Over the Paris Area (ESQUIF) campaign in the Ile-de-France region. Journal of Geophysical Research 108, 8560. https://doi.org/10.1029/2001JD001421

EPRI, 1999. Organic aerosol partition module documentation, technical report. Palo Alto, California.

Favez, O., 2016. Impact de la combustion de biomasse sur les concentrations de PM10 (programme CARA - hiver 2014-2015), Polluants particulaires et caractérisation chimique. INERIS.

Favez, O., Weber, S., Petit, J.-E., Alleman, L.Y., Albinet, A., Riffault, V., Chazeau, B., Amodeo, T., Salameh, D., Zhang, Y., Srivastava, D., Samaké, A., Aujay-Plouzeau, R., Papin, A., Bonnaire, N., Boullanger, C., Chatain, M., Chevrier, F., Detournay, A., Dominik-Sègue, M., Falhun, R., Garbin, C., Ghersi, V., Grignion, G., Levigoureux, G., Pontet, S., Rangognio, J., Zhang, S., Besombes, J.-L., Conil, S., Uzu, G., Savarino, J., Marchand, N., Gros, V., Marchand, C., Jaffrezo, J.-L., Leoz-Garziandia, E., 2021. Overview of the French Operational Network for In Situ Observation of PM Chemical Composition and Sources in Urban Environments (CARA Program). Atmosphere 12, 207. https://doi.org/10.3390/atmos12020207

Forstner, H.J.L., Flagan, R.C., Seinfeld, J.H., 1997. Secondary Organic Aerosol from the Photooxidation of Aromatic Hydrocarbons: Molecular Composition. Environ. Sci. Technol. 31, 1345–1358. https://doi.org/10.1021/es9605376

Fountoukis, C., Nenes, A., 2007. ISORROPIA II: a computationally efficient thermodynamic equilibrium model for K^+-Ca^{2+}-Mg^{2+}-NH_4^+-Na^+-SO_4^2 $^-$-NO_3^--Cl^--H_2O aerosols. Atmospheric Chemistry and Physics 7, 4639–4659. https://doi.org/10.5194/acp-7-4639-2007

Fraser, M.P., Lakshmanan, K., 2000. Using Levoglucosan as a Molecular Marker for the Long-Range Transport of Biomass Combustion Aerosols. Environ. Sci. Technol. 34, 4560–4564. https://doi.org/10.1021/es991229l

Fredenslund, A., Jones, R.L., Prausnitz, J.M., 1975. Group-contribution estimation of activity coefficients in nonideal liquid mixtures. AIChE Journal 21, 1086–1099. https://doi.org/10.1002/aic.690210607

Golly, B., Waked, A., Weber, S., Samake, A., Jacob, V., Conil, S., Rangognio, J., Chrétien, E., Vagnot, M.-P., Robic, P.-Y., Besombes, J.-L., Jaffrezo, J.-L., 2019. Organic markers and OC source apportionment for seasonal variations of PM2.5 at 5 rural sites in France.

Atmospheric Environment 198, 142–157. https://doi.org/10.1016/j.atmosenv.2018.10.027

Gonçalves, C., Alves, C., Pio, C., 2012. Inventory of fine particulate organic compound emissions from residential wood combustion in Portugal. Atmospheric Environment 50, 297–306. https://doi.org/10.1016/j.atmosenv.2011.12.013

Haeffelin, M., Barthès, L., Bock, O., Boitel, C., Bony, S., Bouniol, D., Chepfer, H., Chiriaco, M., Cuesta, J., Delanoë, J., Drobinski, P., Dufresne, J.-L., Flamant, C., Grall, M., Hodzic, A., Hourdin, F., Lapouge, F., Lemaître, Y., Mathieu, A., Morille, Y., Naud, C., Noël, V., O'Hirok, W., Pelon, J., Pietras, C., Protat, A., Romand, B., Scialom, G., Vautard, R., 2005. SIRTA, a ground-based atmospheric observatory for cloud and aerosol research. Annales Geophysicae 23, 253–275.

Hallquist, M., Wenger, J.C., Baltensperger, U., Rudich, Y., Simpson, D., Claeys, M., Dommen, J., Donahue, N.M., George, C., Goldstein, A.H., Hamilton, J.F., Herrmann, H., Hoffmann, T., Iinuma, Y., Jang, M., Jenkin, M.E., Jimenez, J.L., Kiendler-Scharr, A., Maenhaut, W., McFiggans, G., Mentel, T.F., Monod, A., Prevot, A.S.H., Seinfeld, J.H., Surratt, J.D., Szmigielski, R., Wildt, J., 2009. The formation, properties and impact of secondary organic aerosol: current and emerging issues. Atmos. Chem. Phys 9, 5155–5236. https://doi.org/10.5194/acp-9-5155-2009

Hankett, J.M., Collin, W.R., Chen, Z., 2013. Molecular Structural Changes of Plasticized PVC after UV Light Exposure. J. Phys. Chem. B 117, 16336–16344. https://doi.org/10.1021/jp409254y

Hatch, L.E., Rivas-Ubach, A., Jen, C.N., Lipton, M., Goldstein, A.H., Barsanti, K.C., 2018. Measurements of I/SVOCs in biomass-burning smoke using solid-phase extraction disks and two-dimensional gas chromatography. Atmospheric Chemistry and Physics 18, 17801–17817. https://doi.org/10.5194/acp-18-17801-2018

He, X., Huang, X.H.H., Chow, K.S., Wang, Q., Zhang, T., Wu, D., Yu, J.Z., 2018. Abundance and Sources of Phthalic Acids, Benzene-Tricarboxylic Acids, and Phenolic Acids in PM2.5 at Urban and Suburban Sites in Southern China. ACS Earth Space Chem. 2, 147–158. https://doi.org/10.1021/acsearthspacechem.7b00131

Heald, C.L., Kroll, J.H., 2020. The fuel of atmospheric chemistry: Toward a complete description of reactive organic carbon. Science Advances 6, eaay8967. https://doi.org/10.1126/sciadv.aay8967

Hennigan, C.J., Sullivan, A.P., Collett, J.L., Robinson, A.L., 2010. Levoglucosan stability in biomass burning particles exposed to hydroxyl radicals. Geophysical Research Letters 37. https://doi.org/10.1029/2010GL043088

Herich, H., Gianini, M.F.D., Piot, C., Močnik, G., Jaffrezo, J.-L., Besombes, J.-L., Prévôt, A.S.H., Hueglin, C., 2014. Overview of the impact of wood burning emissions on carbonaceous aerosols and PM in large parts of the Alpine region. Atmospheric Environment 89, 64–75. https://doi.org/10.1016/j.atmosenv.2014.02.008

Hobbs, P.J., Webb, J., Mottram, T.T., Grant, B., Misselbrook, T.M., 2004. Emissions of volatile organic compounds originating from UK livestock agriculture. Journal of the Science of Food and Agriculture 84, 1414–1420. https://doi.org/10.1002/jsfa.1810

Hopke, P.K., Dai, Q., Li, L., Feng, Y., 2020. Global review of recent source apportionments for airborne particulate matter. Science of The Total Environment 740, 140091. https://doi.org/10.1016/j.scitotenv.2020.140091

Iinuma, Y., Böge, O., Gräfe, R., Herrmann, H., 2010. Methyl-nitrocatechols: atmospheric tracer compounds for biomass burning secondary organic aerosols. Environmental Science & Technology 44, 8453–8459. https://doi.org/10.1021/es102938a

Kanakidou, M., Seinfeld, J.H., Pandis, S.N., Barnes, I., Dentener, F.J., Facchini, M.C., Dingenen, R.V., Ervens, B., Nenes, A., Nielsen, C.J., 2005. Organic aerosol and global climate modelling: a review. Atmospheric Chemistry and Physics 5, 1053–1123. https://doi.org/10.5194/acp-5-1053-2005

Karagulian, F., Belis, C.A., Dora, C.F.C., Prüss-Ustün, A.M., Bonjour, S., Adair-Rohani, H., Amann, M., 2015. Contributions to cities' ambient particulate matter (PM): A systematic review of local source contributions at global level. Atmospheric Environment 120, 475–483. https://doi.org/10.1016/j.atmosenv.2015.08.087

Kautzman, K.E., Surratt, J.D., Chan, M.N., Chan, A.W.H., Hersey, S.P., Chhabra, P.S., Dalleska, N.F., Wennberg, P.O., Flagan, R.C., Seinfeld, J.H., 2010. Chemical Composition of Gas- and Aerosol-Phase Products from the Photooxidation of Naphthalene. The Journal of Physical Chemistry A 114, 913–934. https://doi.org/10.1021/jp908530s

Kawamura, K., Kaplan, I.R., 1987. Motor exhaust emissions as a primary source for dicarboxylic acids in Los Angeles ambient air. Environ. Sci. Technol. 21, 105–110. https://doi.org/10.1021/es00155a014

Kim, Y., Sartelet, K., Couvidat, F., 2019. Modeling the effect of non-ideality, dynamic mass transfer and viscosity on SOA formation in a 3-D air quality model. Atmospheric Chemistry and Physics Discussions 1–29. https://doi.org/10.5194/acp-2018-177

Kleindienst, T.E., Jaoui, M., Lewandowski, M., Offenberg, J.H., Docherty, K.S., 2012. The formation of SOA and chemical tracer compounds from the photooxidation of naphthalene and its methyl analogs in the presence and absence of nitrogen oxides. Atmospheric Chemistry and Physics 12, 8711–8726. https://doi.org/10.5194/acp-12-8711-2012

Kleindienst, T.E., Jaoui, M., Lewandowski, M., Offenberg, J.H., Lewis, C.W., Bhave, P.V., Edney, E.O., 2007. Estimates of the contributions of biogenic and anthropogenic hydrocarbons to secondary organic aerosol at a southeastern US location. Atmospheric Environment 41, 8288–8300. https://doi.org/10.1016/j.atmosenv.2007.06.045

Kroll, J.H., Seinfeld, J.H., 2008. Chemistry of secondary organic aerosol: Formation and evolution of low-volatility organics in the atmosphere. Atmospheric Environment 42, 3593–3624. https://doi.org/10.1016/j.atmosenv.2008.01.003

Kulmala, M., Laaksonen, A., Pirjola, L., 1998. Parameterizations for sulfuric acid/water nucleation rates. Journal of Geophysical Research: Atmospheres 103, 8301–8307. https://doi.org/10.1029/97JD03718

Lanzafame, G.M., Srivastava, D., Favez, O., Bandowe, B.A.M., Shahpoury, P., Lammel, G., Bonnaire, N., Alleman, L.Y., Couvidat, F., Bessagnet, B., Albinet, A., 2021. One-year measurements of secondary organic aerosol (SOA) markers in the Paris region

(France): Concentrations, gas/particle partitioning and SOA source apportionment. Science of The Total Environment 757, 143921. https://doi.org/10.1016/j.scitotenv.2020.143921

Lauraguais, A., Coeur-Tourneur, C., Cassez, A., Deboudt, K., Fourmentin, M., Choël, M., 2014. Atmospheric reactivity of hydroxyl radicals with guaiacol (2-methoxyphenol), a biomass burning emitted compound: Secondary organic aerosol formation and gas-phase oxidation products. Atmospheric Environment 86, 155–163. https://doi.org/10.1016/j.atmosenv.2013.11.074

Lelieveld, J., Crutzen, P.J., 1991. The role of clouds in tropospheric photochemistry. J Atmos Chem 12, 229–267. https://doi.org/10.1007/BF00048075

Li, Y., Fu, T.-M., Yu, J.Z., Feng, X., Zhang, L., Chen, J., Boreddy, S.K.R., Kawamura, K., Fu, P., Yang, X., Zhu, L., Zeng, Z., 2021. Impacts of Chemical Degradation on the Global Budget of Atmospheric Levoglucosan and Its Use As a Biomass Burning Tracer. Environ. Sci. Technol. 55, 5525–5536. https://doi.org/10.1021/acs.est.0c07313

Locker, H.B., 1988. The use of levoglucosan to assess the environmental impact of residential wood-burning on air quality. Dartmouth College, Hanover, NH.

Lu, C., Wang, X., Li, R., Gu, R., Zhang, Y., Li, W., Gao, R., Chen, B., Xue, L., Wang, W., 2019. Emissions of fine particulate nitrated phenols from residential coal combustion in China. Atmospheric Environment 203, 10–17. https://doi.org/10.1016/j.atmosenv.2019.01.047

Majdi, M., Sartelet, K., Lanzafame, G.M., Couvidat, F., Kim, Y., Chrit, M., Turquety, S., 2019. Precursors and formation of secondary organic aerosols from wildfires in the Euro-Mediterranean region. Atmospheric Chemistry and Physics 19, 5543–5569. https://doi.org/10.5194/acp-19-5543-2019

May, A.A., Levin, E.J.T., Hennigan, C.J., Riipinen, I., Lee, T., Collett, J.L., Jimenez, J.L., Kreidenweis, S.M., Robinson, A.L., 2013. Gas-particle partitioning of primary organic aerosol emissions: 3. Biomass burning. Journal of Geophysical Research: Atmospheres 118, 11,327-11,338. https://doi.org/10.1002/jgrd.50828

May, A.A., Saleh, R., Hennigan, C.J., Donahue, N.M., Robinson, A.L., 2012a. Volatility of Organic Molecular Markers Used for Source Apportionment Analysis: Measurements and Implications for Atmospheric Lifetime. Environ. Sci. Technol. 46, 12435–12444. https://doi.org/10.1021/es302276t

May, A.A., Saleh, R., Hennigan, C.J., Donahue, N.M., Robinson, A.L., 2012b. Volatility of Organic Molecular Markers Used for Source Apportionment Analysis: Measurements and Implications for Atmospheric Lifetime. Environ. Sci. Technol. 46, 12435–12444. https://doi.org/10.1021/es302276t

McDonald, J.D., Zielinska, B., Fujita, E.M., Sagebiel, J.C., Chow, J.C., Watson, J.G., 2000. Fine Particle and Gaseous Emission Rates from Residential Wood Combustion. Environmental Science & Technology 34, 2080–2091. https://doi.org/10.1021/es9909632

Nalin, F., Golly, B., Besombes, J.-L., Pelletier, C., Aujay-Plouzeau, R., Verlhac, S., Dermigny, A., Fievet, A., Karoski, N., Dubois, P., Collet, S., Favez, O., Albinet, A., 2016. Fast oxidation processes from emission to ambient air introduction of aerosol emitted by residential

log wood stoves. Atmospheric Environment 143, 15–26. https://doi.org/10.1016/j.atmosenv.2016.08.002

Nozière, B., Kalberer, M., Claeys, M., Allan, J., D'Anna, B., Decesari, S., Finessi, E., Glasius, M., Grgić, I., Hamilton, J.F., Hoffmann, T., Iinuma, Y., Jaoui, M., Kahnt, A., Kampf, C.J., Kourtchev, I., Maenhaut, W., Marsden, N., Saarikoski, S., Schnelle-Kreis, J., Surratt, J.D., Szidat, S., Szmigielski, R., Wisthaler, A., 2015. The Molecular Identification of Organic Compounds in the Atmosphere: State of the Art and Challenges. Chem. Rev. 115, 3919–3983. https://doi.org/10.1021/cr5003485

Oja, V., Suuberg, E.M., 1999. Vapor Pressures and Enthalpies of Sublimation of D -Glucose, D - Xylose, Cellobiose, and Levoglucosan. Journal of Chemical & Engineering Data 44, 26– 29. https://doi.org/10.1021/je980119b

Olariu, R.I., Klotz, B., Barnes, I., Becker, K.H., Mocanu, R., 2002. FT–IR study of the ring-retaining products from the reaction of OH radicals with phenol, o-, m-, and p-cresol. Atmospheric Environment 36, 3685–3697.

Pandis, S.N., Wexler, A.S., Seinfeld, J.H., 1993. Secondary organic aerosol formation and transport - II. Predicting the ambient secondary organic aerosol size distribution. 4TMOS. ENVIRON. 27, 2403–2416. https://doi.org/10.1016/0960-1686(93)90408-Q

Parshintsev, J., Ruiz-Jimenez, J., Petäjä, T., Hartonen, K., Kulmala, M., Riekkola, M.-L., 2011. Comparison of quartz and Teflon filters for simultaneous collection of size-separated ultrafine aerosol particles and gas-phase zero samples. Analytical and Bioanalytical Chemistry 400, 3527–3535. https://doi.org/10.1007/s00216-011-5041-0

Passant, N.R., 2002. Speciation of UK emissions of non-methane volatile organic compounds (No. AEAT/ENV/R/0545). Oxon.

Pouet, J.-C., Gautier, A., 2013. Etude sur le chauffage domestique au bois: marches et approvisionnement. ADEME.

Pratap, V., Bian, Q., Kiran, S.A., Hopke, P.K., Pierce, J.R., Nakao, S., 2019. Investigation of levoglucosan decay in wood smoke smog-chamber experiments: The importance of aerosol loading, temperature, and vapor wall losses in interpreting results. Atmospheric Environment 199, 224–232. https://doi.org/10.1016/j.atmosenv.2018.11.020

Puxbaum, H., Caseiro, A., Sánchez-Ochoa, A., Kasper-Giebl, A., Claeys, M., Gelencsér, A., Legrand, M., Preunkert, S., Pio, C.A., 2007. Levoglucosan levels at background sites in Europe for assessing the impact of biomass combustion on the European aerosol background. J Geophisical Research 112, D23S05. https://doi.org/10.1029/2006JD008114

Robinson, A.L., Donahue, N.M., Shrivastava, M.K., Weitkamp, E.A., Sage, A.M., Grieshop, A.P., Lane, T.E., Pierce, J.R., Pandis, S.N., 2007. Rethinking Organic Aerosols: Semivolatile Emissions and Photochemical Aging. Science 315, 1259–1262. https://doi.org/10.1126/science.1133061

Roldin, P., Ehn, M., Kurtén, T., Olenius, T., Rissanen, M.P., Sarnela, N., Elm, J., Rantala, P., Hao, L., Hyttinen, N., Heikkinen, L., Worsnop, D.R., Pichelstorfer, L., Xavier, C., Clusius, P., Öström, E., Petäjä, T., Kulmala, M., Vehkamäki, H., Virtanen, A., Riipinen, I., Boy, M.,

2019. The role of highly oxygenated organic molecules in the Boreal aerosol-cloud-climate system. Nat Commun 10, 1–15. https://doi.org/10.1038/s41467-019-12338-8

Salvador, C.M.G., Tang, R., Priestley, M., Li, L.J., Tsiligiannis, E., Le Breton, M., Zhu, W., Zeng, L., Wang, H., Yu, Y., Hu, M., Guo, S., Hallquist, M., 2020. Ambient Nitro-Aromatic Compounds – Biomass Burning versus Secondary Formation in rural China. Atmos. Chem. Phys. https://doi.org/doi.org/10.5194/acp-2020-899

Schauer, J.J., Kleeman, M.J., Cass, G.R., Simoneit, B.R.T., 2001. Measurement of Emissions from Air Pollution Sources. 3. C_1 –C_{29} Organic Compounds from Fireplace Combustion of Wood. Environmental Science & Technology 35, 1716–1728. https://doi.org/10.1021/es001331e

Schauer, J.J., Rogge, W.F., Hildemann, L.M., Mazurek, M.A., Cass, G.R., Simoneit, B.R.T., 1996. Source apportionment of airborne particulate matter using organic compounds as tracers. Atmospheric Environment 30, 3837–3855. https://doi.org/10.1016/1352-2310(96)00085-4

Schmidl, C., Bauer, H., Dattler, A., Hitzenberger, R., Weissenboeck, G., Marr, I.L., Puxbaum, H., 2008. Chemical characterisation of particle emissions from burning leaves. Atmospheric Environment 42, 9070–9079. https://doi.org/10.1016/j.atmosenv.2008.09.010

Shrivastava, M., Cappa, C.D., Fan, J., Goldstein, A.H., Guenther, A.B., Jimenez, J.L., Kuang, C., Laskin, A., Martin, S.T., Ng, N.L., Petaja, T., Pierce, J.R., Rasch, P.J., Roldin, P., Seinfeld, J.H., Shilling, J., Smith, J.N., Thornton, J.A., Volkamer, R., Wang, J., Worsnop, D.R., Zaveri, R.A., Zelenyuk, A., Zhang, Q., 2017. Recent advances in understanding secondary organic aerosol: Implications for global climate forcing: Advances in Secondary Organic Aerosol. Reviews of Geophysics 55, 509–559. https://doi.org/10.1002/2016RG000540

Simoneit, B.R., Schauer, J.J., Nolte, C.G., Oros, D.R., Elias, V.O., Fraser, M.P., Rogge, W.F., Cass, G.R., 1999. Levoglucosan, a tracer for cellulose in biomass burning and atmospheric particles. Atmospheric Environment 33, 173–182.

Simoneit, B.R.T., Medeiros, P.M., Didyk, B.M., 2005. Combustion Products of Plastics as Indicators for Refuse Burning in the Atmosphere. Environ. Sci. Technol. 39, 6961–6970. https://doi.org/10.1021/es050767x

Srivastava, D., Daellenbach, K.R., Zhang, Y., Bonnaire, N., Chazeau, B., Perraudin, E., Gros, V., Lucarelli, F., Villenave, E., Prévôt, A.S.H., El Haddad, I., Favez, O., Albinet, A., 2021. Comparison of five methodologies to apportion organic aerosol sources during a PM pollution event. Science of The Total Environment 757, 143168. https://doi.org/10.1016/j.scitotenv.2020.143168

Srivastava, D., Favez, O., Bonnaire, N., Lucarelli, F., Haeffelin, M., Perraudin, E., Gros, V., Villenave, E., Albinet, A., 2018a. Speciation of organic fractions does matter for aerosol source apportionment. Part 2: Intensive short-term campaign in the Paris area (France). Science of The Total Environment 634, 267–278. https://doi.org/10.1016/j.scitotenv.2018.03.296

Srivastava, D., Favez, O., Perraudin, E., Villenave, E., Albinet, A., 2018b. Comparison of Measurement-Based Methodologies to Apportion Secondary Organic Carbon (SOC) in

PM2.5: A Review of Recent Studies. Atmosphere 9, 452. https://doi.org/10.3390/atmos9110452

Srivastava, D., Favez, O., Petit, J.-E., Zhang, Y., Sofowote, U.M., Hopke, P.K., Bonnaire, N., Perraudin, E., Gros, V., Villenave, E., Albinet, A., 2019. Speciation of organic fractions does matter for aerosol source apportionment. Part 3: Combining off-line and on-line measurements. Science of The Total Environment 690, 944–955. https://doi.org/10.1016/j.scitotenv.2019.06.378

Srivastava, D., Tomaz, S., Favez, O., Lanzafame, G.M., Golly, B., Besombes, J.-L., Alleman, L.Y., Jaffrezo, J.-L., Jacob, V., Perraudin, E., Villenave, E., Albinet, A., 2018c. Speciation of organic fraction does matter for source apportionment. Part 1: A one-year campaign in Grenoble (France). Science of The Total Environment 624, 1598–1611. https://doi.org/10.1016/j.scitotenv.2017.12.135

Teil, M.J., Blanchard, M., Chevreuil, M., 2006. Atmospheric fate of phthalate esters in an urban area (Paris-France). Science of The Total Environment 354, 212–223. https://doi.org/10.1016/j.scitotenv.2004.12.083

Verlhac, S., Favez, O., Albinet, A., 2013. Interlaboratory comparison organized for the European laboratories involved in the analysis of levoglucosan and its isomers. LCSQA.

Vestreng, V., 2003. Review and Revision. Emission data reported to CLRTAP Tech. Rep. EMEP MSW-W,Norvegian Meteorological Institute, Oslo, Norway.

Wang, X., Gu, R., Wang, L., Xu, W., Zhang, Y., Chen, B., Li, W., Xue, L., Chen, J., Wang, W., 2017. Emissions of fine particulate nitrated phenols from the burning of five common types of biomass. Environmental Pollution 230, 405–412. https://doi.org/10.1016/j.envpol.2017.06.072

Wilson, J., Octaviani, M., Bandowe, B.A.M., Wietzoreck, M., Zetzsch, C., Pöschl, U., Berkemeier, T., Lammel, G., 2020. Modeling the Formation, Degradation, and Spatiotemporal Distribution of 2-Nitrofluoranthene and 2-Nitropyrene in the Global Atmosphere. Environ. Sci. Technol. 54, 14224–14234. https://doi.org/10.1021/acs.est.0c04319

Xavier, C., Rusanen, A., Zhou, P., Dean, C., Pichelstorfer, L., Roldin, P., Boy, M., 2019. Aerosol Mass yields of selected Biogenic Volatile Organic Compounds - a theoretical study with near explicit gas-phase chemistry. Atmospheric Chemistry and Physics Discussions 1–26. https://doi.org/10.5194/acp-2019-424

Xie, M., Hannigan, M.P., Barsanti, K.C., 2014. Gas/Particle Partitioning of 2-Methyltetrols and Levoglucosan at an Urban Site in Denver. Environmental Science & Technology 48, 2835–2842. https://doi.org/10.1021/es405356n

Yang, B., Zhang, H., Wang, Y., Zhang, P., Shu, J., Sun, W., Ma, P., 2016. Experimental and theoretical studies on gas-phase reactions of NO3 radicals with three methoxyphenols: Guaiacol, creosol, and syringol. Atmospheric Environment 125, 243–251. https://doi.org/10.1016/j.atmosenv.2015.11.028

Yee, L.D., Kautzman, K.E., Loza, C.L., Schilling, K.A., Coggon, M.M., Chhabra, P.S., Chan, M.N., Chan, A.W.H., Hersey, S.P., Crounse, J.D., Wennberg, P.O., Flagan, R.C., Seinfeld, J.H., 2013. Secondary organic aerosol formation from biomass burning intermediates:

phenol and methoxyphenols. Atmospheric Chemistry and Physics 13, 8019–8043. https://doi.org/10.5194/acp-13-8019-2013

Yttri, K.E., Schnelle-Kreis, J., Maenhaut, W., Abbaszade, G., Alves, C., Bjerke, A., Bonnier, N., Bossi, R., Claeys, M., Dye, C., Evtyugina, M., García-Gacio, D., Hillamo, R., Hoffer, A., Hyder, M., Iinuma, Y., Jaffrezo, J.-L., Kasper-Giebl, A., Kiss, G., López-Mahia, P.L., Pio, C., Piot, C., Ramirez-Santa-Cruz, C., Sciare, J., Teinilä, K., Vermeylen, R., Vicente, A., Zimmermann, R., 2015. An intercomparison study of analytical methods used for quantification of levoglucosan in ambient aerosol filter samples. Atmos. Meas. Tech. 8, 125–147. https://doi.org/10.5194/amt-8-125-2015

Zhang, Q., Jimenez, J.L., Canagaratna, M.R., Allan, J.D., Coe, H., Ulbrich, I., Alfarra, M.R., Takami, A., Middlebrook, A.M., Sun, Y.L., Dzepina, K., Dunlea, E., Docherty, K., DeCarlo, P.F., Salcedo, D., Onasch, T., Jayne, J.T., Miyoshi, T., Shimono, A., Hatakeyama, S., Takegawa, N., Kondo, Y., Schneider, J., Drewnick, F., Borrmann, S., Weimer, S., Demerjian, K., Williams, P., Bower, K., Bahreini, R., Cottrell, L., Griffin, R.J., Rautiainen, J., Sun, J.Y., Zhang, Y.M., Worsnop, D.R., 2007. Ubiquity and dominance of oxygenated species in organic aerosols in anthropogenically-influenced Northern Hemisphere midlatitudes. Geophysical Research Letters 34, L13801. https://doi.org/10.1029/2007GL029979

Zhang, Q., Jimenez, J.L., Canagaratna, M.R., Ulbrich, I.M., Ng, N.L., Worsnop, D.R., Sun, Y., 2011. Understanding atmospheric organic aerosols via factor analysis of aerosol mass spectrometry: a review. Anal Bioanal Chem 401, 3045–3067. https://doi.org/10.1007/s00216-011-5355-y

Zhang, Y., Favez, O., Petit, J.-E., Canonaco, F., Truong, F., Bonnaire, N., Crenn, V., Amodeo, T., Prévôt, A.S.H., Sciare, J., Gros, V., Albinet, A., 2019. Six-year source apportionment of submicron organic aerosols from near-continuous highly time-resolved measurements at SIRTA (Paris area, France). Atmospheric Chemistry and Physics 19, 14755–14776. https://doi.org/10.5194/acp-19-14755-2019

Zhang, J., He, X., Gao, Y., Zhu, S., Jing, S., Wang, H., Yu, J.Z., Ying, Q., 2021. Estimation of Aromatic Secondary Organic Aerosol Using a Molecular Tracer—A Chemical Transport Model Assessment. Environ. Sci. Technol. 55, 12882–12892. https://doi.org/10.1021/acs.est.1c03670

Ziemann, P.J., Atkinson, R., 2012. Kinetics, products, and mechanisms of secondary organic aerosol formation. Chemical Society Reviews 41, 6582. https://doi.org/10.1039/c2cs35122f

Zuend, A., Marcolli, C., Booth, A.M., Lienhard, D.M., Soonsin, V., Krieger, U.K., Topping, D.O., McFiggans, G., Peter, T., Seinfeld, J.H., 2011. New and extended parameterization of the thermodynamic model AIOMFAC: calculation of activity coefficients for organic-inorganic mixtures containing carboxyl, hydroxyl, carbonyl, ether, ester, alkenyl, alkyl, and aromatic functional groups. Atmos. Chem. Phys. 11, 9155–9206. https://doi.org/10.5194/acp-11-9155-2011

Zuend, A., Marcolli, C., Peter, T., Seinfeld, J.H., 2010. Computation of liquid-liquid equilibria and phase stabilities: implications for RH-dependent gas/particle partitioning of organic-inorganic aerosols. Atmospheric Chemistry and Physics 10, 7795–7820. https://doi.org/10.5194/acp-10-7795-2010

Zuend, A., Seinfeld, J.H., 2012. Modeling the gas-particle partitioning of secondary organic aerosol: the importance of liquid-liquid phase separation. Atmospheric Chemistry and Physics 12, 3857–3882. https://doi.org/10.5194/acp-12-3857-2012